Bordetella pertussis adenylate cyclase toxin disrupts functional integrity of bronchial epithelial layers

Shakir Hasan[1$], Nikhil Nitin Kulkarni[2$*], Arni Asbjarnarson[2], Irena Linhartova[1], Radim Osicka[1], Peter Sebo[1#], Gudmundur H. Gudmundsson[2#].

[1] Institute of Microbiology of the CAS, v.v.i., Prague, Czech Republic.

[2] Biomedical Center, University of Iceland, Reykjavík, Iceland.

#Address correspondence to Peter Sebo (sebo@biomed.cas.cz) or Gudmundur Hrafn Gudmundsson (ghrafn@hi.is).

[$]S.H. and N.N.K. contributed equally to this work.

* Present address: Department of Dermatology, University of California, San Diego, USA

ABSTRACT

Airway epithelium restricts penetration of inhaled pathogens into the underlying tissue and plays a crucial role in innate immune defense against respiratory infections. The whooping cough agent, *Bordetella pertussis,* adheres to ciliated cells of human airway epithelium and subverts its defense functions through the action of secreted toxins and other virulence factors. We have examined the impact of *B. pertussis* infection and of adenylate cyclase toxin (CyaA) action on the functional integrity of air-liquid interface (ALI)-cultured human bronchial epithelial cells. *B. pertussis* adhesion to the apical surface of polarized pseudostratified VA10 cell layers provoked disruption of tight junctions and caused drop of the trans-epithelial electrical resistance (TEER). The reduction of TEER depended on the capacity of the secreted CyaA toxin to elicit cAMP signaling in epithelial cells through its adenylyl cyclase enzyme activity. Both purified CyaA and cAMP signaling drugs triggered decrease of TEER of VA10 cell layers. Toxin-produced cAMP signaling caused actin cytoskeleton rearrangement and induced mucin 5AC production and IL-6 secretion, while inhibiting IL-17A-induced secretion of the IL-8 chemokine and of the antimicrobial peptide beta defensin-2. These results indicate that CyaA toxin activity compromises the barrier and innate immune functions of *Bordetella*-infected airway epithelia.

KEYWORDS: *B. pertussis*, airway epithelia, CyaA, tight junctions, antimicrobial peptides, immunomodulatory cytokines

INTRODUCTION

Despite availability and world-wide use of pertussis vaccines, whooping cough (pertussis) remains the least controlled vaccine-preventable infectious disease. The illness is primarily caused by the Gram-negative coccobacillus *Bordetella pertussis* and about 10% of milder whooping cough cases are caused by the related organism *B. parapertussis*$_{hu}$. The agent is transmitted by aerosolized droplets (1, 2) and upon inhalation the bacteria bind to the ciliated epithelial cells along the airway. With progressing proliferation, *B. pertussis* can reach the bronchioles and lung alveoli. It was proposed that a large fraction of live bacteria recovered from infected mouse lungs may have been residing inside alveolar macrophages (3). *B. pertussis* was also repeatedly found to survive and proliferate inside human macrophages (4, 5) and within epithelial cells infected *ex vivo* (6, 7). Moreover, two month after an infant patient was diagnosed with whooping cough disease, persisting *B. pertussis* antigens could still be detected in its airway epithelial cells (8). However, it remains unclear whether intracellular survival of *B. pertussis* within host epithelial cells, or in alveolar macrophages, plays any role in the pathophysiology of whooping cough disease, which can last for up to three months.

B. pertussis produces a number of virulence factors that enable it to overcome the innate and adaptive immune defense functions of airway mucosa. Several types of adhesins produced in parallel (*e.g*. fimbriae, filamentous hemagglutinin (FHA), pertactin) appear to mediate adhesion of the bacteria to human ciliated epithelia or macrophage cells. *B. pertussis* further produces several complement resistance factors and at least two potent immunomodulatory toxins, the pertussis toxin (PTX) and the adenylate cyclase toxin-hemolysin (CyaA). These play a major role in subversion of host innate

and adaptive immune defense. The underexplored Type III Secretion System (T3SS) of *Bordetellae* then delivers immunomodulatory (BopN) and cytotoxic (BteA/BopC) effectors into host cells, but the mechanism by which the T3SS contributes to pathogenesis of *B. pertussis* infections remains unknown (2, 9, 10).

The adenylate cyclase toxin-hemolysin (ACT, AC-Hly or CyaA) plays a particular role in the initial phases of *B. pertussis* infection (11). CyaA belongs to the Repeats-in-toxin (RTX) family of proteins and it consists of an N-terminal cell invasive adenylate cyclase enzyme domain (~384 residues) that is fused to a pore-forming RTX cytolysin (Hly) moiety (~1322 residues) (12, 13). Through binding to the CD11b subunit of the complement receptor 3 ($\alpha_M\beta_2$ integrin, CD11b/CD18, or Mac-1), the CyaA toxin primarily targets host myeloid phagocytes (14). It inserts into their cell membrane and upon forming a transmembrane conduit for influx of extracellular Ca^{2+} ions, CyaA delivers its N-terminal adenylate cyclase (AC) domain into the cytosol of cells (15). There the AC enzyme is activated by calmodulin and catalyzes massive and unregulated conversion of ATP into the second messenger molecule 3',5'-cyclic adenosine monophosphate (cAMP) (16). cAMP signaling then instantly ablates the bactericidal functions of the myeloid phagocytes, such as the oxidative burst and opsonophagocytic killing of bacteria by neutrophils and macrophages (16-20). In parallel, the Hly moiety oligomerizes into cation-selective pores and permeabilizes cells for efflux of cytosolic K^+ ions, activating MAPK signaling (21).

With a reduced efficacy, CyaA can bind, penetrate and intoxicate by cAMP a variety of other host cell types that do not express CR3 ($CD11b^-$ cells), such as erythrocytes or epithelial cells (14, 22, 23). However, very little is known about how

CyaA action affects the function of airway epithelial linings. CyaA appears to translocate rather inefficiently through the apical membrane of polarized epithelial cells (24), but it could be delivered into epithelial cells by bacterial outer membrane vesicles (25). This raises the possibility that cAMP produced by OMV-delivered CyaA might compromise tight junction integrity and enable the free secreted toxin to access the basolateral side of the layer, from where it can rather efficiently invade epithelial cells (24). Moreover, *B. pertussis* bacteria were recently shown to secrete high amounts of CyaA in the presence of calcium and albumin, as present in human respiratory secretions (26-28). This indicates that intoxication of airway epithelial cells by CyaA-produced cAMP likely plays a more important role in the pathophysiology of *B. pertussis* infections than previously anticipated.

The airway epithelium represents the first line of innate immune defense against respiratory pathogens (29). The secreted mucins form a protective gel layer over the epithelial surface that traps inhaled particles and microorganisms, enabling their removal by the mucociliary escalator (29, 30). Expression of Toll-like receptors (e.g. TLR2 and TLR4) and of the endotoxin receptor CD14 enables the airway epithelial cells to sense the presence of components released by infecting bacteria, such as the LPS and lipoproteins/lipopeptides, triggering secretion of cytokines and antimicrobial peptides (31, 32). Cytokines secreted by the epithelia can then act as chemoattractants, as pro/anti-inflammatory regulators, or as maturation signals for intraepithelial immune cells (32, 33). Tight packing of the epithelial cells through tight junctions plays a key role in the barrier function of the epithelial layer, preventing penetration of inhaled particles and microbes into the underlying tissue (34).

We have previously shown that when grown in air-liquid interface cultures (ALI), the human bronchial epithelial cell line VA10 can form a pseudo-stratified epithelium that forms functional tight junctions, secretes IL-8 and antimicrobial peptides, and responds to bacterial components (35-38). Here, we used this model to analyze the effects of *B. pertussis* CyaA toxin action on the barrier function and immune response of bronchial epithelium. We show that *B. pertussis* infection and especially the elevation of cAMP by CyaA toxin compromises tight junction integrity and enhances mucin production, while modulating cytokine and antimicrobial peptide secretion by polarized airway epithelial cells.

MATERIALS AND METHODS

Reagents and antibodies. Bronchial/Tracheal epithelial cell growth medium (B/TEGM) was obtained from Cell applications, USA. Dulbecco's Modified Eagles Medium: Nutrient mixture F-12 (DMEM/F12) was purchased from Thermo Fisher, USA. Serum substitute Ultroser G was obtained from PALL Life Sciences, USA. Antibody against zonula occludens-1 (ZO-1; polyclonal Rabbit), junctional adhesion molecule A (JAMA; polyclonal rabbit), claudin-1 (monoclonal mouse), claudin-4 (polyclonal rabbit) and Alexa Flour 488 conjugated anti-mouse IgG were purchased from Thermo Scientific, USA. Glyceraldehyde 3-phosphate dehydrogenase (GAPDH) (polyclonal rabbit), E-cadherin (polyclonal rabbit), and anti-Mouse IgG HRP antibodies were all from Santa Cruz Biotechnologies (USA). Anti-*Bordetella* serum (rabbit polyclonal) was a generous gift from Dr. Branislav Vecerek. Cy-3 conjugated anti-rabbit antibody was obtained from Sigma-Aldrich, USA. Rabbit polyclonal anti-cAMP antibody for competitive ELISA was obtained from Genscript, USA. Transwell permeable filter supports (0.4 µm pore size, Polyester membrane) were bought from Corning Costar Corporation, USA. F-actin staining was done with Alexa Fluor 488 phalloidin (Molecular Probes, Thermo Scientific, USA). Anti-human ZO-1 antibody was also obtained from BD biosciences. Radio-Immunoprecipitation Assay (RIPA) buffer was purchased from Sigma Aldrich, USA; and used along with protease inhibitor cocktail and phosphatase inhibitors obtained from Life Technologies, USA. Micro BCA Protein Assay kit for protein estimation was obtained from Thermo Fisher Scientific, USA. Recombinant human IL-17A and human beta defensin-2 (hBD-2) standard TMB ELISA development kit were obtained from Peprotech, UK. Human CXCL8/IL-8 and human IL-6 ELISA kits were

purchased from R&D systems, UK. FITC Annexin V Apoptosis Detection Kit I was obtained from BD Biosciences, USA. Human MUC5AC ELISA kit was obtained from LifeSpan BioSciences, Inc; USA. Mouse monoclonal anti-CyaA antibody (9D4) was kindly provided by Erik L. Hewlett (University of Virginia School of Medicine, Charlottesville, USA). A mouse poly-clonal serum recognizing the S1 subunit of pertussis toxin was a kind gift of Nicole Guiso, Institut Pasteur, Paris, France and a mAb recognizing the N-terminal region of filamentous hemagglutinin was a kind gift of Camille Locht, Institut Pasteur Lille, France. Pertactin polyclonal rabbit serum was generated in SPF rabbits by immunization with recombinant purified P69 form of pertactin.

Production and purification of CyaA. CyaA and the CyaA-AC$^-$ toxoid (with AC enzyme activity ablated by a GlySer dipeptide insert between residues 188 and 189) were produced in the *E. coli* strain XL1-Blue (Stratagene, La Jolla, CA). The proteins were purified by a combination of ion exchange chromatography on DEAE-Sepharose and hydrophobic chromatography on Phenyl-Sepharose, as described in detail elsewhere (20, 39) and were stored in 50 mM Tris pH 8.0, 8 M urea, and 2 mM $CaCl_2$ (TUC buffer) at -20 °C.

Cell Culture and Air-Liquid Interface (ALI). An E6/E7 viral oncogene immortalized human bronchial epithelial cell line VA10 was cultured as described previously (40). Briefly, the cells were maintained in B/TEGM with antibiotic-antimycotic solution (0.1 mg/ml streptomycin, 100 U/ml penicillin, and 0.25 µg/ml amphotericin) at 37 °C and 5% CO_2. ALI cultures were set up on transwell permeable filter supports. Cells were seeded in B/TEGM medium with antibiotic-antimycotic solution. Three to four

days after seeding, medium was changed to DMEM/F12 supplemented with 2% Ultroser G and antibiotic-antimycotic solution on both apical and basolateral sides. Three to four days later the medium was removed from the apical surface. The cells were cultured at the air–liquid interface for 21 days, with media changed every second day. Mature ALI cultures (VA10 cell layers) that generated transepithelial resistance (TEER) of at least 350 $\Omega.cm^2$ were used for further studies.

Bacterial strains and co-culture experiments. The *Bordetella pertussis* Tohama I (WT) isolate was obtained as the CIP 81.32 strain from the Collection of Institute Pasteur, Paris, France. The *B. pertussis* Δ*cyaA* mutant, carrying an in-frame deletion of the *cyaA* open reading frame on the chromosome (Δ*cyaA*) was constructed using the pSS4245 allelic exchange vector (generously provided by Dr. S. Stibitz), as described in detail elsewhere (19). *B. pertussis* strains were grown on BGA plates (Bordet-Gengou agar, Becton Dickinson) containing 15% defibrinated sheep blood. Colonies from a fresh plate were resuspended to OD_{600} = 0.2 in modified Stainer-Scholte medium (supplemented with 1g/l of casamino acids and 1 g/l 2-hydroxypropyl-β-cyclodextrin). The bacteria were grown overnight at 37 °C with shaking to OD_{600} = 1 (2 x 10^9 colony forming units (CFU)/ml). Bacterial suspensions were diluted in DMEM/F12 with 10% FCS and no antibiotics to ~2 x 10^7 CFU/ml and incubated further at 37 °C for 1 hour before addition to the apical side of VA10 cell layers at a multiplicity of infection (MOI) of 50 (unless stated otherwise). It was controlled by Western blotting that there was no observable difference in the production of FHA, PTX, and pertactin between the WT *B. pertussis* and the CyaA-deficient *B. pertussis ΔcyaA* strains (Fig. S1).

Trans-epithelial electrical resistance (TEER). TEER was measured with a Millicell-ERS volt-ohm meter (Millipore, USA). For experiments with *B. pertussis,* the bacteria in DMEM/F12 with 10% FCS and no antibiotics were added to the apical side of VA10 cell layers. CyaA or CyaA-AC$^-$ was diluted in DMEM/F12 with 2% UltroserG and antibiotic-antimycotic solution. Background resistance of empty transwell filters was subtracted. The TEER was calculated as $\Omega.cm^2$.

In control experiments forskolin (5 µg/ml) or 100 µM di-butyryl cAMP (Santacruz Biotechnologies, USA) were dissolved in Dimethyl Sulfoxide (DMSO) according to manufacturer's instructions. The final concentration of DMSO was kept at 0.1% v/v or less and did not affect the expression of target genes or TEER at this concentration.

Adenylate cyclase assay. Adenylate cyclase (AC) activities were measured as previously described in the presence of 1µM calmodulin (41). One unit of AC activity corresponds to 1 µmol of cAMP per minute at 30 °C. For determination of CyaA penetration across the cell layer, 10 µl of the basal chamber medium was assayed at 24 hours after apical *B. pertussis* infection.

Apoptosis assay. VA10 cell layers were treated with TUC buffer, CyaA, or CyaA-AC$^-$ as mentioned above for 24 hours at 37 °C and the cell layers were washed twice with PBS-EDTA. Cells were detached with Trypsin-EDTA for 7-10 minutes at 37 °C and 10% Fetal calf serum was added. The cells were washed twice and assayed for apoptosis by the FITC Annexin V Apoptosis Detection Kit I according to manufacturer's instructions.

Immunofluorescent staining. For confocal microscopy, cells on transwell support membranes were washed twice with ice-cold PBS and fixed using cold

methanol (-20 °C) for 15 minutes, permeabilized with acetone (-20 °C) for 50 seconds and rinsed with methanol again. Sequential rehydration was carried out using 70 %, 50 %, and 30 % methanol at 4 °C for 5 minutes each. After fixation, the cell layers were washed with PBS and blocked with 5 % BSA in PBS for 30 minutes at room temperature. After fixation and blocking, the membrane with cell layer was extracted from the polystyrene support using sharp forceps. The cells were probed with the primary antibody diluted in 2% BSA in PBS for 60 minutes, washed three times with PBS and stained in 2 % BSA with fluorochrome-conjugated secondary antibody along with DAPI (1 µg/ml) for 30 minutes. Finally, the cell layers were washed with PBS, rinsed once with distilled water, and mounted on a clean microscopic slide in Vectashield mounting medium (Vector laboratories). Immunofluorescent images were obtained using Olympus FV-1000 confocal microscope (Olympus Corporation, Tokyo, Japan). Tight Junction Organization Rate (TiJOR) was calculated using an ImageJ macro (42), to evaluate the damage to tight junction networks. TiJOR (entire image) was calculated by evaluating the entire representative images obtained from confocal microscopy. TiJOR for *Bordetella* foci was calculated by evaluating the specific areas of images where the bacteria were localized. Correspondingly, an area of untreated cell layers was arbitrarily chosen as a control to best represent the tight junction network. The starting area (60 x 60 units) and parameters (20 polygons, 4 steps) of evaluation were kept constant through all '*Bordetella* foci' evaluations. Mucin 5AC and F-actin staining was quantified using Image J.

cAMP assay. ALI-grown VA10 cell layers were treated with indicated concentrations of CyaA (0.1, 0.5, 5 µg/ml) added apically or basally for 30 minutes at 37

°C in DMEM with 10% FCS. The reaction was stopped by lysing the cells with 0.2% Tween in 50 mM HCl. cAMP levels in the lyzate were determined by a competitive ELISA as mentioned elsewhere (43, 44). cAMP concentrations were normalized to total protein content determined using a Micro BCA protein assay kit (Bio-Rad, Rockford, USA).

Mucin 5AC ELISA. Intracellular mucin 5AC production was measured using the Human MUC5AC ELISA kit (LifeSpan BioSciences, Inc; USA) according to manufacturer's instructions. Toxin treated VA10 cell layers were detached from the membrane, lysed by a sequential freeze-thaw procedure (4 times, freezing in liquid nitrogen, thawing in 37 °C water bath), centrifuged, and the supernatant was used for ELISA.

Cytokines and hBD-2 measurement. IL-17A, CyaA, or both, were added in DMEM/F12 with 2% UltroserG and antibiotic-antimycotic solution to the basolateral side of VA10 cell layers. Basolateral supernatants were collected after 24 hours of incubation, and cytokine/hBD-2 levels were determined by ELISA according to manufacturer's instruction. Concentrations were calculated from calibration curves using the MasterPlex ReaderFit software (Hitachi SolutionsAmerica, San Diego, CA, USA) by generating four parameter logistic curve-fit.

RNA isolation and quantitative real time PCR. Total RNA was isolated using the NucleoSpin RNA kit (Macherey-Nagel, Germany, Cat.No. 740955) and quantified using a Nanodrop spectrophotometer (Thermo Scientific, USA). Isolated RNA was reverse transcribed into first strand cDNA using High capacity cDNA reverse transcription kit according to manufacturer's instructions (Life Technologies, USA). The

cDNA was quantified with Power SYBR green Universal PCR master mix (Applied Biosystems, USA) on a 7500 Real time PCR machine (Applied Biosystems, USA). Ubiquitin C (UBC) gene was used as a reference in all the quantitative real time PCR (q-RT PCR) experiments. A non-template control was included in all experiments. Some primers were designed using Primer3 or Perl primer (Table S1). All additional primers were purchased from Integrated DNA technologies (PrimeTimeTM predesigned qPCR Assays) and were used at a final concentration of 500 nM according to manufacturer's instructions, unless stated otherwise. All primers gave a single PCR product as evaluated with the aid of a melting curve. The default cycling conditions were as followed: 1) initial denaturation; 95°C for 10 min followed by 40 cycles of: 2) denaturation step; 95°C for 15 sec and 3) annealing/extension step: 60°C for 1 min. The $2^{(-\Delta\Delta CT)}$ Livak method was utilized for calculating fold difference over untreated control (45).

Western blot analysis. CyaA-treated cell layers were washed three times with ice-cold PBS, incubated for 30 min on ice with complete RIPA lysis buffer. The lyzate was cleared at 12,000 rpm for 10 min at 4°C and its protein content was determined by the Bradford method (Bio-Rad, USA). The proteins were separated by SDS-PAGE (4-12% gradient Bis-Tris SDS gels, Life Technologies, USA) and transferred onto a PVDF membrane (Millipore, USA) using the NuPage blotting kit (Life Technologies, USA). Upon blocking with 5% non-fat skimmed milk in 1x PBS with 0.05% Tween 20 (PBST), the membranes were probed with primary antibodies diluted 1:200-1:1000 in PBST with 0.5% non-fat skimmed milk or 2% bovine serum albumin, according to recommendation of antibody manufacturers. Upon repeated washing, the detected proteins were

revealed with 1:10,000-diluted horseradish peroxidase (HRP)-linked secondary antibody (Sigma Aldrich, USA) using the Pierce ECL plus chemiluminescence substrate (Thermo Scientific, USA) and an Image Quant LAS 4000 station (GE Healthcare, USA).

Statistical analysis. Normally distributed results for q-RT PCR experiments are represented as means and standard error of the means from at least three independent experiments. For comparison of differences between two groups, the unpaired Student's t-test was used. For comparison of more than two groups, one-way ANOVA test was used. For comparison of two different categorical independent variables, two-way ANOVA was used. Tukey's test or Dunnett's test were used for post hoc analysis. P value of less than 0.05 was considered statistically significant. All the statistical analysis was performed with the Prism 6 software (Graph Pad, USA). The axis was split in some graphs to facilitate accurate representation of the trends.

RESULTS

***B. pertussis* infection compromises tight junction integrity of differentiated epithelial cell layers.** We first assessed the impact of *B. pertussis* infection on tight junction integrity of differentiated ALI-grown VA10 bronchial epithelial cell layers. As documented in Fig. 1A, upon bacterial infection of the apical side at an approximate multiplicity of infection (MOI) of 50:1, the trans-epithelial electrical resistance (TEER) of the pseudostratified VA10 cell layers dropped progressively over 24 hours. Compared to mock-treated cell layers, the TEER was significantly reduced already after 12 hours of infection with the wild-type *B. pertussis* strain that produced an active CyaA toxin. Infection with the CyaA-deficient Δ*cyaA* strain caused a delayed and slower drop of TEER of the VA10 layer, which was not significantly different from the spontaneous decrease of the TEER of mock-treated VA10 layers. At 24 hours after infection, the difference in the magnitude of TEER decrease provoked by the WT and the *ΔcyaA* strains was statistically significant. Therefore, we examined the tight junction integrity of VA10 layers after 24 hours of infection by confocal immunofluorescence microscopy. As shown in Fig. 1B, in untreated VA10 cell layers the staining for the zonula occludens 1 protein (ZO-1) revealed a normal ZO-1 network that is characteristic for functional tight junctions. Upon infection by both *B. pertussis* WT and *B. pertussis ΔcyaA* bacteria, the apical ZO-1 network was disrupted and delocalized. As determined by calculation of the Tight Junction Organization Rate (TiJOR) for representative series of entire confocal images (Fig. 1C), an infection by CyaA-secreting WT bacteria caused a more pronounced ZO-1 network disruption than an infection by the *ΔcyaA* strain. The ZO-1 network was particularly disrupted in the areas designated as *Bordetella* foci, where

313 bacteria were adhering and growing in clusters (Fig. 1D). Again, a stronger decrease of
314 TiJOR was reproducibly observed in the foci of CyaA-secreting WT bacteria than
315 beneath the foci of the *ΔcyaA* mutant. This indicated that action of the CyaA toxin was
316 specifically involved in disruption of the barrier function of the infected VA10 epithelial
317 cell layers.

318 **CyaA-produced cAMP signaling disrupts the barrier function of VA10**
319 **layers.** In line with the previous observation of Eby et al. (2010) on T84 intestinal
320 epithelial cells, CyaA elevated cAMP more efficiently when acting from the basolateral
321 side than from the apical side of the polarized VA10 bronchial epithelial cells (Fig. 2A).
322 Basal side exposure to increasing CyaA concentrations yielded up to ten-fold higher
323 levels of cytosolic cAMP than what was generated by equal amounts of CyaA applied to
324 the apical side. At the highest used CyaA concentration of 5 µg/mL, translocation of the
325 toxin across the basolateral membrane resulted in up to 2489±1659 pmoles of
326 cAMP/mg of cellular protein, as compared to 158±41 pmoles of cAMP/mg protein when
327 equal CyaA amounts were applied apically (Fig. 2A). In line with that, treatment with 500
328 ng/ml of CyaA from the basolateral side triggered a steady decrease of TEER of the
329 polarized VA10 layer already within the first hour from addition (Fig. 2B). In contrast,
330 while the AC enzyme activity of CyaA in the used medium was rather stable over
331 prolonged incubation times (Fig. S2), a reduction in TEER could only be observed after
332 more than five hours from addition of equal amounts of CyaA to the apical side.

333 The CyaA-triggered decrease of TEER was clearly due to CyaA-elicited cAMP
334 signaling and was not due to toxin-induced cell death, since the viability of CyaA-treated
335 VA10 cells was not affected over the incubation period (Fig. S3). Moreover, no TEER

decrease was observed upon treatment with equal concentrations of the catalytically inactive CyaA-AC$^-$ toxoid that is unable to convert ATP to cAMP (Fig. 2C). Indeed, the CyaA-elicited TEER decrease could be mimicked by treatment of the VA10 cells with Forskolin (FSK, 5 µg/mL), an activator of the cellular adenylyl cyclase enzyme isoforms, or by the cell-permeable cAMP analogue dibutyryl-cAMP (db-cAMP, 100 µM). Compared to the DMSO solvent control, these cAMP signaling-eliciting compounds provoked a 70 % or 50 % reduction of TEER (Fig. 2D).

It was important to test if upon infection of the apical surface of the polarized epithelial layer by *B. pertussis* the secreted CyaA could cross the pseudostratified cell layer to penetrate cells from their basal side. Therefore, we assessed the amounts of CyaA accumulating in the basal chamber medium of transwells with VA10 cell layers infected by *B. pertussis* from the apical side. As shown in Fig. 2E for two MOI, detectable amounts of adenylate cyclase enzyme activity (CyaA) were found in the basal chamber medium after 24 hours of infection of the apical surface and cAMP accumulated in the infected cells (Fig. 2F).

The CyaA-produced cAMP signaling did not significantly alter the expression of genes encoding the tight junction proteins, such as ZO-1 (*TJP1*), occludin (*OCLN*), and claudin-1 (*CLDN1*) (Fig. 3A). However, as revealed by immunodetection in whole cell lyzates (Fig. 3B), the action of CyaA provoked a progressive decrease of the detectable amounts of several tight junction marker proteins, such as occludin, ZO-1, junctional adhesion molecule A (JAMA), and claudin-1. In particular, the detected amounts of occludin and ZO-1 proteins were strongly decreased already within 1 hour after toxin addition to cell layers. The JAMA and claudin-1 protein amounts decreased noticeably

only after 24 hours of incubation with the toxin, whereas the amounts of claudin-4 and of the adherens junction marker E-cadherin were almost not affected (Fig. 3B). The CyaA-produced cAMP signaling thus provoked a rapid and selective degradation of some but not all of the tight junction proteins.

In line with the drop of occludin and ZO-1 protein amounts, a clear reduction of ZO-1 network organization in CyaA-treated cell layers was observed by confocal microscopy (Fig. 3C). CyaA treatment resulted in reduced TiJOR, whereas CyaA-AC$^-$ did not affect tight junction integrity (Fig. 3D), confirming that CyaA compromised the tight junction integrity through cAMP signaling.

CyaA induces mucin production and actin reorganization in polarized VA10 cells. The mucus layer plays an important role in anti-microbial innate defense mechanisms, where mucin 5AC and mucin 5B are the predominant mucin species secreted by airway epithelia. As shown in Fig. 4A, CyaA-produced cAMP signaling strongly enhanced expression of the *Muc5AC* and *Muc5B* genes, as did cAMP elevation by forskolin (Fig. S4A). As detected by mucin 5AC-specific ELISA (Fig. 4B) and confocal immunofluorescence imaging (Fig. 4C and 4D), the CyaA-treated VA10 cell layers contained increased amounts of intracellularly accumulated mucin 5AC. Moreover, in line with previous observations made on neuroblastoma, epithelial or monocytic cells exposed to CyaA (46-48), the CyaA-elicited cAMP signaling provoked reorganization of the actin cytoskeleton in polarized VA10 cells (Fig. 5A and 5B).

cAMP signaling of CyaA differentially affects production of antimicrobial peptides and cytokines. *B. pertussis* infection of cultured non-polarized bronchial epithelial cells was previously shown to result in a pro-inflammatory alteration of

382 expression profiles of NFκB-regulated genes, but the role of CyaA in these alterations
383 was not analyzed (49). Therefore, we used qPCR to investigate the impact of CyaA
384 toxin action on expression of genes encoding cytokines and antimicrobial
385 peptides/proteins that are known to play an important role in innate immune functions of
386 the epithelial layers (Fig. 6). In the examined set of genes encoding antimicrobial
387 peptides/proteins (Fig. 6A to 6F), such as cathelicidin (CAMP), human beta defensin-1
388 (hBD-1), human beta defensin-2 (hBD-2), lysozyme (LZY), secretory leukocyte
389 peptidase inhibitor (SLPI) and lactoferrin (LTF), a significant downregulation of
390 expression of the hBD2-encoding gene was observed already within 1 hour after CyaA
391 addition to the basolateral side of the VA10 layers (Fig. 6C). In contrast, the CyaA-
392 induced changes of the mRNA levels for CAMP, hBD1, LZY, SLPI and LTF proteins
393 was not significant (Fig. 6A, B, D, E, and F).

394 CyaA action resulted in a statistically significant suppression of expression of
395 genes for the proinflammatory cytokines tumor necrosis factor-alpha (TNF-α),
396 interleukin-1 beta (IL-1β), and interleukin 8 (IL-8). The effect was noticeable within 1
397 hour from CyaA addition and it was most pronounced after 24 hours of toxin treatment
398 (Fig. 6G, 6I and 6K). On the contrary, within 1 hour from toxin addition, the action of
399 CyaA provoked some enhancement of expression of genes coding for interleukin-1
400 alpha (IL-1α), interleukin-6 (IL-6), and interleukin-10 (IL-10). However, the expression of
401 these genes returned to basal levels, or below them, within 24 hours from toxin addition
402 (Fig. 6H, 6J and 6L). All these effects reflected the cAMP signaling capacity of CyaA
403 and could be elicited by drugs elevating cAMP levels in cells, while the CyaA-AC$^-$ toxoid
404 had no effect (Figure S4B, S4C, S4D, and S6).

CyaA modulates IL-6, IL-8, and hBD-2 secretion in VA10 cell layers. To verify that the altered gene expression levels translated into altered levels of secreted cytokines and antimicrobial peptides, the cells were treated with 500 ng/mL of CyaA in the presence or absence of IL-17A. This cytokine was shown to activate the innate immune functions of epithelial cells (50), such as the expression of the *TNF* gene (TNF-α, Fig. S5A), or of the *DEFB4A* gene (hBD-2, Fig. S5B). Indeed, CyaA action could eliminate this enhancing effect of IL-17A treatment at least in part, whereas CyaA-AC$^-$ could not (Fig. S5).

To corroborate the impact of CyaA action on production of the canonical epithelial cytokines IL-6 and IL-8 (51), and of the antimicrobial peptide hBD-2 (50), the VA10 cell layers were treated with 500 ng/mL of CyaA in the presence or absence of stimulation with 100 ng/mL of recombinant IL-17A. The levels of IL-6, IL-8, and hBD-2 secreted into the basolateral supernatant of the cultures after 24 hours of treatment were then determined by ELISA. As shown in Fig. 7, CyaA treatment triggered an enhanced secretion of IL-6 even in the absence of any stimulation and the effect was potentiated in the presence of IL-17A (Fig. 7A). In contrast, CyaA action alone had no effect on the amount of secreted IL-8, while this was enhanced upon stimulation with IL-17A and CyaA action interfered only marginally with the enhancing effect of IL-17A stimulation (Fig. 7B). Similarly, despite of a reduced expression of the defensin gene (*cf.* Fig. 6C), CyaA activity did not significantly reduce the basal amount of hBD-2 secreted from cells within 24 hours of toxin action. However, in the presence of CyaA the enhancing effect of IL-17A on secretion of hBD-2 was suppressed, showing that CyaA activity counteracts the IL-17A-induced hBD-2 production by epithelial cells (Fig. 7C).

DISCUSSION

We used here the model of ALI-grown differentiated human bronchial epithelial VA10 cells to assess the impact of *B. pertussis* infection on airway epithelial layers, placing a particular emphasis on the contribution and role of CyaA in compromising of the epithelial barrier and innate immunity functions.

B. pertussis is an obligatory human pathogen with no known environmental reservoir. The mouse model of respiratory infection replicates certain aspects of human pertussis pathophysiology, but does not reproduce the full spectrum of the disease symptoms. These symptoms can be rather truly reproduced in the recently developed baboon infection model, the use of which is limited by high cost and low numbers of animals available per test group (52). The need for detailed understanding of the infection thus calls for the development of alternative *in vitro* models for controlled studies on molecular aspects of *B*. *pertussis* interaction with the airway epithelium.

Mammalian epithelial cells grown as submerged monolayers may lack important phenotypic and physiological features of the polarized differentiated human airway epithelial tissue. Indeed, highly differentiated primary human airway epithelial cell layers and cultured HBE-2 bronchial epithelial cells were recently be used for infection with *B. pertussis* to study the role of fimbriae in bacterial adherence to ciliated cells (53). We used here VA10 epithelial cells, polarized and differentiated at an air-liquid interface (ALI), which form pseudostratified epithelial layers with apicobasal polarity, functional tight junctions and TEER, the hallmarks of epithelial barrier function (40, 54). A previous study from our group showed that infection by the opportunistic pathogen *Pseudomonas aeruginosa* provokes complete loss of TEER, where the barrier function of ALI-grown

VA10 layers is obliterated by a coordinated action of numerous secreted cytotoxic factors (37). In contrast, *B. pertussis* infection produced a relatively modest reduction in TEER of the epithelial layer and this process involved the action of CyaA. Our results on polarized VA10 cells confirm the observations of Eby et al. (2010) that polarized T84 cell monolayers were rather resistant to cAMP intoxication by CyaA applied to the apical side. Indeed, CyaA penetrated polarized cells more efficiently across the basolateral membrane (*cf.* Fig. 2A). Importantly, we have observed here that CyaA secreted by *B. pertussis* attached to the apical side can cross the pseudostratified epithelial layer and act on cells from their basal side. This indicates that in the course of natural *Bordetellae* infections the CyaA toxin action compromises the barrier function of airway epithelia.

The cell polarity effect of CyaA action on epithelial cell layers is intriguing and deserves further investigation. One of its plausible explanations could be the specific localization of phosphodiesterase 4D to the cytosolic side of the apical membrane. Indeed, phosphodiesterase 4 is regulated by the cAMP-activated protein kinase A (PKA) and forms a cAMP diffusion barrier on the apical side of airway epithelia (55). Alternatively, an unfavorable composition of the apical membrane might present a particular obstacle for efficient membrane insertion and translocation of CyaA into cytosol of epithelial cells. Delivery of the AC enzyme of CyaA into cytosol of cells was previously shown to depend on the presence of cholesterol-rich lipid microdomains through which the AC domain of membrane-inserted CyaA can accomplish the translocation across the lipid bilayer into the cytosolic compartment to catalyze formation of cAMP (15). The apparently higher efficacy of CyaA translocation through the basal membrane might then potentially be due to its lipid composition and higher

474 cholesterol or glycolipid content. On airway epithelial cells the expression of the
475 proteinaceous receptor for CyaA (CD11b/CD18) has not been observed (56, 57) and in
476 the absence of CD11b/CD18 expression the toxin might be binding to surface
477 expressed glycosylated structures, such as the gangliosides clustered in the membrane
478 microdomains (43, 58-60). This hypothesis would go well with the observed apicobasal
479 polarity in the distribution of receptors on airway epithelia (61, 62).

480 We show here that CyaA secreted by *B. pertussis* bacteria adhering to the apical
481 surface can cross the epithelial layer as the functionality of tight junctions gets
482 compromised. It remains to be established if this is due to the sole action of the CyaA
483 toxin. *B. pertussis* produces a number of other virulence factors that might affect tight
484 junction integrity of epithelial layers. It is conceivable that pertussis toxin, tracheal
485 cytotoxin, type III secretion effectors, or dermonecrotic toxin action may cooperate with
486 CyaA in compromising tight junction functions. Moreover, in the context of bacterial
487 infection, the CyaA toxin or the pertussis toxin delivered through the apical membrane
488 by outer membrane vesicles (25, 63) might also be involved in attenuation of tight
489 junction integrity. Such attenuation of tight junctions would open the paracellular route
490 for the free secreted CyaA to access the basal side of the cell layer; intoxicate epithelial
491 cells effectively and thus generate a positive feedback loop of sustained elevation of
492 cAMP and disruption of tight junction integrity.

493 We show here that CyaA-provoked loss of TEER is accompanied by decrease of
494 detectable amounts of several tight junction proteins, whereas their mRNA expression
495 levels are not significantly affected. This indicates that CyaA-provoked degradation of
496 those proteins. Similar reduction in levels of ZO-1 and occludin has also been observed

upon treatment of Caco-2 cell layers with *Staphylococcus aureus* α-toxin that permeabilizes cellular membrane and enables influx of extracellular calcium ions into cells (64). Indeed, elevation of intracellular Ca^{2+} concentration due to ionomycin was shown to cause drop in TEER (65-67). Translocation of the AC domain polypeptide across the cell membrane is itself accompanied by calcium influx and in certain cell types the CyaA-generated cAMP can open the L-type calcium channels (68, 69). CyaA oligomerizes into pores that mediate efflux of potassium ions, as does the α-toxin. On the other hand, almost no impact on TEER and tight junction protein localization was observed in VA10 cells upon treatment with the CyaA-AC$^-$toxoid (*cf.* Fig. 3), while the toxoid still causes a spike of calcium influx into cells and triggers potassium efflux from cells (68, 70, 71). Furthermore, the effects of CyaA action could largely be mimicked by cAMP elevation in cells exposed to forskolin or to db-cAMP, a cell-permeable cAMP analogue. It can thus be concluded that deregulated signaling of CyaA-produced cAMP was the dominant mechanism by which CyaA provoked loss of tight junction integrity of VA10 layers. However, this was not complete when the cells were treated with forskolin or db-cAMP. This indicates that also ATP depletion triggered by CyaA may have been involved in the disruption of tight junction integrity upon prolonged exposure of cells to CyaA. Indeed, Eby et al. (2012) have observed that 500 ng/mL of CyaA could cause ATP depletion in epithelial cells and a loss of tight junction integrity following ATP depletion was previously observed (72, 73).

A further element that might be contributing to loss of TEER and barrier function of the CyaA-treated epithelial layer likely was the cAMP-induced reorganization of actin and cell shape change. CyaA activity was previously shown to promote cell shape

changes in rat alveolar epithelial cells (47). Moreover, CyaA action through transient inactivation of RhoA (48), was shown to cause massive actin cytoskeleton rearrangements and membrane ruffling in macrophages, where Rho activity was shown to be important for the maintenance of the barrier function of epithelia (74).

In this respect, it is noteworthy that elevation of cellular cAMP can have contrasting effects on tight junction function, depending on the cell/tissue type. For example, cAMP at certain levels promotes localization of occludin and ZO-1 to tight junctions in Caco-2 cells (75). Further, CyaA toxin action on innate immune functions of the polarized epithelium comprised the transcriptional upregulation of mucin genes, which has also been seen upon infection with *B. pertussis* (49). Our results show a clear cAMP-mediated increase of amounts of the goblet cell marker mucin 5AC in VA10 cell layers. A cAMP-mediated increase in mucin secretion has been reported previously (76) and it is plausible to speculate that CyaA action could promote differentiation of p63 positive basal cells (phenotype of VA10 cells) into mucin-producing goblet-like cells, as seen upon IL-13 treatment (54). Enhanced mucin production might then be supporting *B. pertussis* infection and transmission, as the bacteria exploit mucin as a binding substrate (49, 77) and are transmitted in mucus containing aerosol droplets (78).

Another effect of CyaA action on the VA10 cell layers consists of modulation of transcription of genes encoding important cytokines and antimicrobial peptides. CyaA treatment resulted in pronounced downregulation of the *DEFB4A* gene coding for hBD-2 already at 1 hour post CyaA treatment and the secretion of hBD-2 was reduced to basal level in the presence of CyaA even upon concomitant stimulation by IL-17A (*cf.* Fig. 7C). Since it has been shown that *B. pertussis* is susceptible to bacteriostatic action of

hBD-2 (79), the suppression of hBD-2 production by CyaA may represent an important contribution to overcoming of innate immune mechanisms of the epithelia by *B. pertussis*.

The other effects of CyaA action comprised enhanced secretion of IL-6 from epithelial cells, as observed previously (80) and decrease of IL-17A-induced secretion of IL-8. The effects on transcription of genes encoding the TNF-α, IL-10, IL-1β, or IL-1α cytokines were statistically significant but their biological relevance remains to be corroborated. Many of the above-mentioned genes are modulated by the nuclear factor kappa-B (NF-kB) (81). For example, the hBD-2 gene has three NF-kB binding sites in its promoter region (82) and NF-kB activation mediates the initial transcriptional response in epithelial cells infected by *B. pertussis* (49). On the other hand, cAMP signaling can selectively modulate NF-kB activity and can yield both pro-inflammatory and anti-inflammatory responses that are highly tissue/gene-dependent (83). Our results show that cAMP signaling can upregulate expression of the genes encoding IL-6 and mucin 5AC, known to be positively regulated by NF-kB (84, 85); whereas it downregulates the transcription of genes encoding hBD-2 and IL-1β, which are also controlled by NF-kB (82, 86). This complexity of regulation is due to modulatory effects of the cAMP/PKA-activated signaling pathways on the transcriptional co-activators that are directly controlled by the cAMP response element binding protein (CREB) (87). It has been shown that PKA phosphorylated CREB can indirectly inhibit NF-kB by competing for its co-activator, the CREB-binding protein (CBP) (88). Expression of genes encoding mucin 5AC and IL-6 has been described to be dually regulated by CREB and NF-kB

565 (89, 90). Hence, the strength and duration of the signal and tissue/gene specificity will
566 decide if the expression of a certain gene is upregulated or downregulated.

567 IL-17A is an important pro-inflammatory cytokine secreted by activated T cells
568 (Th17). It signals through the IL-17 receptor of epithelial cells and stimulates production
569 of important cytokines, such as IL-6 and IL-8 (51), or of antimicrobial peptides, like hBD-
570 2 (50). Our results suggest that although IL-17 would be produced by the immune cells
571 arriving to the site of *B. pertussis* infection, the action of CyaA may be skewing the
572 response of epithelial cells to such IL-17 stimulation. It would potentiate IL-17A-induced
573 IL-6 secretion (*cf.* Fig. 7A) but suppress the IL-17A-induced hBD-2 production.
574 Moreover, CyaA action caused only a modest inhibition of the IL-17A-induced
575 production of the neutrophil attracting chemokine IL-8. This must not necessarily be a
576 problem for the infecting bacterium, as cAMP intoxication by the secreted CyaA
577 paralyzes the bactericidal functions of neutrophils very efficiently (18).

578 In conclusion, we present here a model of *B. pertussis* infection of polarized
579 human bronchial epithelial cells forming pseudostratified layers, where specific effects
580 on the function of bronchial epithelium could be attributed to CyaA toxin activity. This
581 will facilitate deciphering of the molecular mechanisms of action of *B. pertussis*
582 virulence factors on airway epithelia.

583

ACKNOWLEDGEMENTS

We are grateful to Dr. Branislav Vecerek for providing anti-*Bordetella* serum. Dr. Christine Terryn graciously provided the macro for evaluating TiJOR. Blanka Jurkova is acknowledged for excellent technical help. This work was supported by a grant to Gudmundur Hrafn Gudmundsson from Icelandic Centre for Research (RANNIS) and the University of Iceland Research Fund. Further support came from the Czech CSF grants GA15-09157S (RO), GA13-14547S (PS), the NV16-28126A (PS), the LM2015064 grant from the Ministry of Education, Youth and Sports of the Czech Republic (RO), and the 'Modernization and support the research activities of the national infrastructure for translational medicine EATRIS-CZ' project (CZ.02.1.01/0.0/0.0/16_013/0001818) funded by Operational Programme Research, Development and Education.

REFERENCES

1. Kilgore PE, Salim AM, Zervos MJ, Schmitt HJ. 2016. Pertussis: Microbiology, Disease, Treatment, and Prevention. Clin Microbiol Rev 29:449-86.
2. Melvin JA, Scheller EV, Miller JF, Cotter PA. 2014. Bordetella pertussis pathogenesis: current and future challenges. Nat Rev Microbiol 12:274-88.
3. Saukkonen K, Cabellos C, Burroughs M, Prasad S, Tuomanen E. 1991. Integrin-mediated localization of Bordetella pertussis within macrophages: role in pulmonary colonization. J Exp Med 173:1143-9.
4. Friedman RL, Nordensson K, Wilson L, Akporiaye ET, Yocum DE. 1992. Uptake and intracellular survival of Bordetella pertussis in human macrophages. Infect Immun 60:4578-85.
5. Lamberti YA, Hayes JA, Perez Vidakovics ML, Harvill ET, Rodriguez ME. 2010. Intracellular trafficking of Bordetella pertussis in human macrophages. Infect Immun 78:907-13.
6. Lamberti Y, Gorgojo J, Massillo C, Rodriguez ME. 2013. Bordetella pertussis entry into respiratory epithelial cells and intracellular survival. Pathog Dis 69:194-204.
7. Bassinet L, Gueirard P, Maitre B, Housset B, Gounon P, Guiso N. 2000. Role of adhesins and toxins in invasion of human tracheal epithelial cells by Bordetella pertussis. Infect Immun 68:1934-41.
8. Paddock CD, Sanden GN, Cherry JD, Gal AA, Langston C, Tatti KM, Wu KH, Goldsmith CS, Greer PW, Montague JL, Eliason MT, Holman RC, Guarner J, Shieh WJ, Zaki SR. 2008. Pathology and pathogenesis of fatal Bordetella pertussis infection in infants. Clin Infect Dis 47:328-38.
9. de Gouw D, Diavatopoulos DA, Bootsma HJ, Hermans PW, Mooi FR. 2011. Pertussis: a matter of immune modulation. FEMS Microbiol Rev 35:441-74.
10. Fennelly NK, Sisti F, Higgins SC, Ross PJ, van der Heide H, Mooi FR, Boyd A, Mills KH. 2008. Bordetella pertussis expresses a functional type III secretion system that subverts protective innate and adaptive immune responses. Infect Immun 76:1257-66.
11. Weiss AA, Hewlett EL, Myers GA, Falkow S. 1984. Pertussis toxin and extracytoplasmic adenylate cyclase as virulence factors of Bordetella pertussis. J Infect Dis 150:219-22.
12. Glaser P, Ladant D, Sezer O, Pichot F, Ullmann A, Danchin A. 1988. The calmodulin-sensitive adenylate cyclase of Bordetella pertussis: cloning and expression in Escherichia coli. Mol Microbiol 2:19-30.
13. Sebo P, Osicka R, Masin J. 2014. Adenylate cyclase toxin-hemolysin relevance for pertussis vaccines. Expert Rev Vaccines 13:1215-27.
14. Guermonprez P, Khelef N, Blouin E, Rieu P, Ricciardi-Castagnoli P, Guiso N, Ladant D, Leclerc C. 2001. The adenylate cyclase toxin of Bordetella pertussis binds to target cells via the alpha(M)beta(2) integrin (CD11b/CD18). J Exp Med 193:1035-44.
15. Bumba L, Masin J, Fiser R, Sebo P. 2010. Bordetella adenylate cyclase toxin mobilizes its beta2 integrin receptor into lipid rafts to accomplish translocation across target cell membrane in two steps. PLoS Pathog 6:e1000901.
16. Vojtova J, Kamanova J, Sebo P. 2006. Bordetella adenylate cyclase toxin: a swift saboteur of host defense. Curr Opin Microbiol 9:69-75.
17. Confer DL, Eaton JW. 1982. Phagocyte impotence caused by an invasive bacterial adenylate cyclase. Science 217:948-50.
18. Cerny O, Anderson KE, Stephens LR, Hawkins PT, Sebo P. 2017. cAMP Signaling of Adenylate Cyclase Toxin Blocks the Oxidative Burst of Neutrophils through Epac-Mediated Inhibition of Phospholipase C Activity. J Immunol 198:1285-1296.

19. Cerny O, Kamanova J, Masin J, Bibova I, Skopova K, Sebo P. 2015. Bordetella pertussis Adenylate Cyclase Toxin Blocks Induction of Bactericidal Nitric Oxide in Macrophages through cAMP-Dependent Activation of the SHP-1 Phosphatase. J Immunol 194:4901-13.
20. Osicka R, Osickova A, Hasan S, Bumba L, Cerny J, Sebo P. 2015. Bordetella adenylate cyclase toxin is a unique ligand of the integrin complement receptor 3. Elife 4:e10766.
21. Masin J, Osicka R, Bumba L, Sebo P. 2015. Bordetella adenylate cyclase toxin: a unique combination of a pore-forming moiety with a cell-invading adenylate cyclase enzyme. Pathog Dis 73:ftv075.
22. Eby JC, Gray MC, Mangan AR, Donato GM, Hewlett EL. 2012. Role of CD11b/CD18 in the process of intoxication by the adenylate cyclase toxin of Bordetella pertussis. Infect Immun 80:850-9.
23. Hanski E. 1989. Invasive adenylate cyclase toxin of Bordetella pertussis. Trends Biochem Sci 14:459-63.
24. Eby JC, Ciesla WP, Hamman W, Donato GM, Pickles RJ, Hewlett EL, Lencer WI. 2010. Selective translocation of the Bordetella pertussis adenylate cyclase toxin across the basolateral membranes of polarized epithelial cells. J Biol Chem 285:10662-70.
25. Donato GM, Goldsmith CS, Paddock CD, Eby JC, Gray MC, Hewlett EL. 2012. Delivery of Bordetella pertussis adenylate cyclase toxin to target cells via outer membrane vesicles. FEBS Lett 586:459-65.
26. Eby JC, Gray MC, Warfel JM, Paddock CD, Jones TF, Day SR, Bowden J, Poulter MD, Donato GM, Merkel TJ, Hewlett EL. 2013. Quantification of the adenylate cyclase toxin of Bordetella pertussis in vitro and during respiratory infection. Infect Immun 81:1390-8.
27. Bumba L, Masin J, Macek P, Wald T, Motlova L, Bibova I, Klimova N, Bednarova L, Veverka V, Kachala M, Svergun DI, Barinka C, Sebo P. 2016. Calcium-Driven Folding of RTX Domain beta-Rolls Ratchets Translocation of RTX Proteins through Type I Secretion Ducts. Mol Cell 62:47-62.
28. Gonyar LA, Gray MC, Christianson GJ, Mehrad B, Hewlett EL. 2017. Albumin, in the presence of calcium, elicits a massive increase in extracellular Bordetella adenylate cyclase toxin. Infect Immun doi:10.1128/IAI.00198-17.
29. Whitsett JA, Alenghat T. 2015. Respiratory epithelial cells orchestrate pulmonary innate immunity. Nat Immunol 16:27-35.
30. Hovenberg HW, Davies JR, Carlstedt I. 1996. Different mucins are produced by the surface epithelium and the submucosa in human trachea: identification of MUC5AC as a major mucin from the goblet cells. Biochem J 318 (Pt 1):319-24.
31. Becker MN, Diamond G, Verghese MW, Randell SH. 2000. CD14-dependent lipopolysaccharide-induced beta-defensin-2 expression in human tracheobronchial epithelium. J Biol Chem 275:29731-6.
32. Weitnauer M, Mijosek V, Dalpke AH. 2016. Control of local immunity by airway epithelial cells. Mucosal Immunol 9:287-98.
33. Stadnyk AW. 1994. Cytokine production by epithelial cells. FASEB J 8:1041-7.
34. Kojima T, Go M, Takano K, Kurose M, Ohkuni T, Koizumi J, Kamekura R, Ogasawara N, Masaki T, Fuchimoto J, Obata K, Hirakawa S, Nomura K, Keira T, Miyata R, Fujii N, Tsutsumi H, Himi T, Sawada N. 2013. Regulation of tight junctions in upper airway epithelium. Biomed Res Int 2013:947072.
35. Asgrimsson V, Gudjonsson T, Gudmundsson GH, Baldursson O. 2006. Novel effects of azithromycin on tight junction proteins in human airway epithelia. Antimicrob Agents Chemother 50:1805-12.
36. Halldorsson S, Asgrimsson V, Axelsson I, Gudmundsson GH, Steinarsdottir M, Baldursson O, Gudjonsson T. 2007. Differentiation potential of a basal epithelial cell line established from human bronchial explant. In Vitro Cell Dev Biol Anim 43:283-9.

37. Halldorsson S, Gudjonsson T, Gottfredsson M, Singh PK, Gudmundsson GH, Baldursson O. 2010. Azithromycin maintains airway epithelial integrity during Pseudomonas aeruginosa infection. Am J Respir Cell Mol Biol 42:62-8.
38. Kulkarni NN, Yi Z, Huehnken C, Agerberth B, Gudmundsson GH. 2015. Phenylbutyrate induces cathelicidin expression via the vitamin D receptor: Linkage to inflammatory and growth factor cytokines pathways. Mol Immunol 63:530-9.
39. Osicka R, Osickova A, Basar T, Guermonprez P, Rojas M, Leclerc C, Sebo P. 2000. Delivery of CD8(+) T-cell epitopes into major histocompatibility complex class I antigen presentation pathway by Bordetella pertussis adenylate cyclase: delineation of cell invasive structures and permissive insertion sites. Infect Immun 68:247-56.
40. Benediktsdottir BE, Arason AJ, Halldorsson S, Gudjonsson T, Masson M, Baldursson O. 2013. Drug delivery characteristics of the progenitor bronchial epithelial cell line VA10. Pharm Res 30:781-91.
41. Ladant D. 1988. Interaction of Bordetella pertussis adenylate cyclase with calmodulin. Identification of two separated calmodulin-binding domains. J Biol Chem 263:2612-8.
42. Terryn C, Sellami M, Fichel C, Diebold MD, Gangloff S, Le Naour R, Polette M, Zahm JM. 2013. Rapid method of quantification of tight-junction organization using image analysis. Cytometry A 83:235-41.
43. Hasan S, Osickova A, Bumba L, Novak P, Sebo P, Osicka R. 2015. Interaction of Bordetella adenylate cyclase toxin with complement receptor 3 involves multivalent glycan binding. FEBS Lett 589:374-9.
44. Karimova G, Pidoux J, Ullmann A, Ladant D. 1998. A bacterial two-hybrid system based on a reconstituted signal transduction pathway. Proc Natl Acad Sci U S A 95:5752-6.
45. Livak KJ, Schmittgen TD. 2001. Analysis of relative gene expression data using real-time quantitative PCR and the 2(-Delta Delta C(T)) Method. Methods 25:402-8.
46. Westrop GD, Campbell G, Kazi Y, Billcliffe B, Coote JG, Parton R, Freer JH, Edwards JG. 1994. A new assay for the invasive adenylate cyclase toxin of Bordetella pertussis based on its morphological effects on the fibronectin-stimulated spreading of BHK21 cells. Microbiology 140 (Pt 2):245-53.
47. Ohnishi H, Miyake M, Kamitani S, Horiguchi Y. 2008. The morphological changes in cultured cells caused by Bordetella pertussis adenylate cyclase toxin. FEMS Microbiol Lett 279:174-9.
48. Kamanova J, Kofronova O, Masin J, Genth H, Vojtova J, Linhartova I, Benada O, Just I, Sebo P. 2008. Adenylate cyclase toxin subverts phagocyte function by RhoA inhibition and unproductive ruffling. J Immunol 181:5587-97.
49. Belcher CE, Drenkow J, Kehoe B, Gingeras TR, McNamara N, Lemjabbar H, Basbaum C, Relman DA. 2000. The transcriptional responses of respiratory epithelial cells to Bordetella pertussis reveal host defensive and pathogen counter-defensive strategies. Proc Natl Acad Sci U S A 97:13847-52.
50. Kao CY, Chen Y, Thai P, Wachi S, Huang F, Kim C, Harper RW, Wu R. 2004. IL-17 markedly up-regulates beta-defensin-2 expression in human airway epithelium via JAK and NF-kappaB signaling pathways. J Immunol 173:3482-91.
51. Tsai HC, Velichko S, Hung LY, Wu R. 2013. IL-17A and Th17 cells in lung inflammation: an update on the role of Th17 cell differentiation and IL-17R signaling in host defense against infection. Clin Dev Immunol 2013:267971.
52. Warfel JM, Merkel TJ. 2014. The baboon model of pertussis: effective use and lessons for pertussis vaccines. Expert Rev Vaccines 13:1241-52.
53. Guevara C, Zhang C, Gaddy JA, Iqbal J, Guerra J, Greenberg DP, Decker MD, Carbonetti N, Starner TD, McCray PB, Jr., Mooi FR, Gomez-Duarte OG. 2016. Highly differentiated human

737 airway epithelial cells: a model to study host cell-parasite interactions in pertussis. Infect Dis
738 (Lond) 48:177-88.
739 54. Arason AJ, Jonsdottir HR, Halldorsson S, Benediktsdottir BE, Bergthorsson JT, Ingthorsson S,
740 Baldursson O, Sinha S, Gudjonsson T, Magnusson MK. 2014. deltaNp63 has a role in maintaining
741 epithelial integrity in airway epithelium. PLoS One 9:e88683.
742 55. Barnes AP, Livera G, Huang P, Sun C, O'Neal WK, Conti M, Stutts MJ, Milgram SL. 2005.
743 Phosphodiesterase 4D forms a cAMP diffusion barrier at the apical membrane of the airway
744 epithelium. J Biol Chem 280:7997-8003.
745 56. Sheppard D. 1998. Airway epithelial integrins: why so many? Am J Respir Cell Mol Biol 19:349-
746 51.
747 57. Sheppard D. 2003. Functions of pulmonary epithelial integrins: from development to disease.
748 Physiol Rev 83:673-86.
749 58. Morova J, Osicka R, Masin J, Sebo P. 2008. RTX cytotoxins recognize beta2 integrin receptors
750 through N-linked oligosaccharides. Proc Natl Acad Sci U S A 105:5355-60.
751 59. Gordon VM, Young WW, Jr., Lechler SM, Gray MC, Leppla SH, Hewlett EL. 1989. Adenylate
752 cyclase toxins from Bacillus anthracis and Bordetella pertussis. Different processes for
753 interaction with and entry into target cells. J Biol Chem 264:14792-6.
754 60. Vojtova J, Kofronova O, Sebo P, Benada O. 2006. Bordetella adenylate cyclase toxin induces a
755 cascade of morphological changes of sheep erythrocytes and localizes into clusters in
756 erythrocyte membranes. Microsc Res Tech 69:119-29.
757 61. Vermeer PD, Einwalter LA, Moninger TO, Rokhlina T, Kern JA, Zabner J, Welsh MJ. 2003.
758 Segregation of receptor and ligand regulates activation of epithelial growth factor receptor.
759 Nature 422:322-6.
760 62. Humlicek AL, Manzel LJ, Chin CL, Shi L, Excoffon KJ, Winter MC, Shasby DM, Look DC. 2007.
761 Paracellular permeability restricts airway epithelial responses to selectively allow activation by
762 mediators at the basolateral surface. J Immunol 178:6395-403.
763 63. Gasperini G, Arato V, Pizza M, Arico B, Leuzzi R. 2017. Physiopathological roles of spontaneously
764 released outer membrane vesicles of Bordetella pertussis. Future Microbiol doi:10.2217/fmb-
765 2017-0064.
766 64. Kwak YK, Vikstrom E, Magnusson KE, Vecsey-Semjen B, Colque-Navarro P, Mollby R. 2012. The
767 Staphylococcus aureus alpha-toxin perturbs the barrier function in Caco-2 epithelial cell
768 monolayers by altering junctional integrity. Infect Immun 80:1670-80.
769 65. Rutten MJ, Cogburn JN, Schasteen CS, Solomon T. 1991. Physiological and cytotoxic effects of
770 Ca(2+) ionophores on Caco-2 paracellular permeability: relationship of 45Ca(2+) efflux to 51 Cr
771 release. Pharmacology 42:156-68.
772 66. Bhat M, Toledo-Velasquez D, Wang L, Malanga CJ, Ma JK, Rojanasakul Y. 1993. Regulation of
773 tight junction permeability by calcium mediators and cell cytoskeleton in rabbit tracheal
774 epithelium. Pharm Res 10:991-7.
775 67. Tai YH, Flick J, Levine SA, Madara JL, Sharp GW, Donowitz M. 1996. Regulation of tight junction
776 resistance in T84 monolayers by elevation in intracellular Ca2+: a protein kinase C effect. J
777 Membr Biol 149:71-9.
778 68. Fiser R, Masin J, Basler M, Krusek J, Spulakova V, Konopasek I, Sebo P. 2007. Third activity of
779 Bordetella adenylate cyclase (AC) toxin-hemolysin. Membrane translocation of AC domain
780 polypeptide promotes calcium influx into CD11b+ monocytes independently of the catalytic and
781 hemolytic activities. J Biol Chem 282:2808-20.
782 69. Otero AS, Yi XB, Gray MC, Szabo G, Hewlett EL. 1995. Membrane depolarization prevents cell
783 invasion by Bordetella pertussis adenylate cyclase toxin. J Biol Chem 270:9695-7.

784 70. Fiser R, Masin J, Bumba L, Pospisilova E, Fayolle C, Basler M, Sadilkova L, Adkins I, Kamanova J,
785 Cerny J, Konopasek I, Osicka R, Leclerc C, Sebo P. 2012. Calcium influx rescues adenylate cyclase-
786 hemolysin from rapid cell membrane removal and enables phagocyte permeabilization by toxin
787 pores. PLoS Pathog 8:e1002580.
788 71. Wald T, Petry-Podgorska I, Fiser R, Matousek T, Dedina J, Osicka R, Sebo P, Masin J. 2014.
789 Quantification of potassium levels in cells treated with Bordetella adenylate cyclase toxin. Anal
790 Biochem 450:57-62.
791 72. Bacallao R, Garfinkel A, Monke S, Zampighi G, Mandel LJ. 1994. ATP depletion: a novel method
792 to study junctional properties in epithelial tissues. I. Rearrangement of the actin cytoskeleton. J
793 Cell Sci 107 (Pt 12):3301-13.
794 73. Brezillon S, Zahm JM, Pierrot D, Gaillard D, Hinnrasky J, Millart H, Klossek JM, Tummler B,
795 Puchelle E. 1997. ATP depletion induces a loss of respiratory epithelium functional integrity and
796 down-regulates CFTR (cystic fibrosis transmembrane conductance regulator) expression. J Biol
797 Chem 272:27830-8.
798 74. Nusrat A, Giry M, Turner JR, Colgan SP, Parkos CA, Carnes D, Lemichez E, Boquet P, Madara JL.
799 1995. Rho protein regulates tight junctions and perijunctional actin organization in polarized
800 epithelia. Proc Natl Acad Sci U S A 92:10629-33.
801 75. Costantini TW, Deree J, Loomis W, Putnam JG, Choi S, Baird A, Eliceiri BP, Bansal V, Coimbra R.
802 2009. Phosphodiesterase inhibition attenuates alterations to the tight junction proteins occludin
803 and ZO-1 in immunostimulated Caco-2 intestinal monolayers. Life Sci 84:18-22.
804 76. Gray T, Nettesheim P, Loftin C, Koo JS, Bonner J, Peddada S, Langenbach R. 2004. Interleukin-
805 1beta-induced mucin production in human airway epithelium is mediated by cyclooxygenase-2,
806 prostaglandin E2 receptors, and cyclic AMP-protein kinase A signaling. Mol Pharmacol 66:337-
807 46.
808 77. Vidakovics ML, Lamberti Y, Serra D, Berbers GA, van der Pol WL, Rodriguez ME. 2007. Iron stress
809 increases Bordetella pertussis mucin-binding capacity and attachment to respiratory epithelial
810 cells. FEMS Immunol Med Microbiol 51:414-21.
811 78. Warfel JM, Beren J, Merkel TJ. 2012. Airborne transmission of Bordetella pertussis. J Infect Dis
812 206:902-6.
813 79. Elahi S, Buchanan RM, Attah-Poku S, Townsend HG, Babiuk LA, Gerdts V. 2006. The host defense
814 peptide beta-defensin 1 confers protection against Bordetella pertussis in newborn piglets.
815 Infect Immun 74:2338-52.
816 80. Bassinet L, Fitting C, Housset B, Cavaillon JM, Guiso N. 2004. Bordetella pertussis adenylate
817 cyclase-hemolysin induces interleukin-6 secretion by human tracheal epithelial cells. Infect
818 Immun 72:5530-3.
819 81. Lawrence T. 2009. The nuclear factor NF-kappaB pathway in inflammation. Cold Spring Harb
820 Perspect Biol 1:a001651.
821 82. Tsutsumi-Ishii Y, Nagaoka I. 2002. NF-kappa B-mediated transcriptional regulation of human
822 beta-defensin-2 gene following lipopolysaccharide stimulation. J Leukoc Biol 71:154-62.
823 83. Gerlo S, Kooijman R, Beck IM, Kolmus K, Spooren A, Haegeman G. 2011. Cyclic AMP: a selective
824 modulator of NF-kappaB action. Cell Mol Life Sci 68:3823-41.
825 84. Libermann TA, Baltimore D. 1990. Activation of interleukin-6 gene expression through the NF-
826 kappa B transcription factor. Mol Cell Biol 10:2327-34.
827 85. Fujisawa T, Velichko S, Thai P, Hung LY, Huang F, Wu R. 2009. Regulation of airway MUC5AC
828 expression by IL-1beta and IL-17A; the NF-kappaB paradigm. J Immunol 183:6236-43.
829 86. Cogswell JP, Godlevski MM, Wisely GB, Clay WC, Leesnitzer LM, Ways JP, Gray JG. 1994. NF-
830 kappa B regulates IL-1 beta transcription through a consensus NF-kappa B binding site and a
831 nonconsensus CRE-like site. J Immunol 153:712-23.

87. Altarejos JY, Montminy M. 2011. CREB and the CRTC co-activators: sensors for hormonal and metabolic signals. Nat Rev Mol Cell Biol 12:141-51.
88. Parry GC, Mackman N. 1997. Role of cyclic AMP response element-binding protein in cyclic AMP inhibition of NF-kappaB-mediated transcription. J Immunol 159:5450-6.
89. Chen Y, Garvin LM, Nickola TJ, Watson AM, Colberg-Poley AM, Rose MC. 2014. IL-1beta induction of MUC5AC gene expression is mediated by CREB and NF-kappaB and repressed by dexamethasone. Am J Physiol Lung Cell Mol Physiol 306:L797-807.
90. Hershko DD, Robb BW, Luo G, Hasselgren PO. 2002. Multiple transcription factors regulating the IL-6 gene are activated by cAMP in cultured Caco-2 cells. Am J Physiol Regul Integr Comp Physiol 283:R1140-8.

FIGURE LEGENDS

FIG 1: ***B. pertussis* infection compromises the tight junction integrity of VA10 bronchial epithelial cell layers.** (A) The apical surfaces of mature ALI-grown VA10 cell layers were infected (MOI = 50) with *B. pertussis* (WT) or its CyaA deficient mutant (Δ*cyaA*). Transepithelial electrical resistance was measured across cell layers at different time intervals. Data represents mean ± SEM (N = 5). ** $p<0.01$, **** $p<0.0001$ compared to untreated; # $p<0.05$ compared to WT (two-way ANOVA). (B) Confocal images of VA10 cell layers treated for 24 hours as in (A), washed, fixed, and stained for ZO-1 (green), *Bordetella* (red) and nuclei (blue). N = 4, scale bar 10 µm. Reconstructed Z stack projections are shown below the main image. (C) Tight Junction Organization Rate (TiJOR) was calculated for representative entire images from four independent experiments using ImageJ; bars represent mean ± SEM, N = 4; * $p<0.05$ according to one-way ANOVA. (D) Areas, where the growth of adhering bacteria was localized, were manually selected and the TiJOR was calculated for images from four independent experiments. An area of untreated cell layers was arbitrarily chosen as a control and analyzed using the same parameters. N = 4, bars represent mean ± SEM; ** $p<0.01$, *** $p<0.001$ according to one-way ANOVA compared to untreated. Untreated cell layers were used as control.

FIG 2: **CyaA-mediated cAMP intoxication disrupts tight junction integrity.** (A) VA10 cell layers were treated with CyaA toxin in DMEM plus 10% FCS from the apical or basolateral side for 30 minutes. Cellular cAMP levels were determined and normalized to cellular protein concentration. N = 3. (B) CyaA (500 ng/ml) or TUC buffer in DMEM/F12 was added to the apical or basolateral side of VA10 cell layers and TEER

was measured at several time intervals of incubation at 37 °C and expressed as relative TEER (%), taking the starting TEER as 100%. N ≥ 3; * p<0.05, **<0.01, ****p<0.0001 compared to TUC (two-way ANOVA). Cell layers were treated with CyaA or the catalytically inactive CyaA-AC$^-$ toxoid (C); 5 µg/ml of forskolin (FSK) or 100 µM dibutyryl-cAMP (db-cAMP) (D); from the basolateral side and TEER was measured at time 0 and 24 hours. The shown values represent mean ± SEM, N = 3. * p<0.05, ** p<0.01 compared to control (Student's t-test). (E) VA10 cell layers were apically infected with *B. pertussis* WT at different MOIs and after 24 hours the amount of adenylate cyclase toxin that reached the basal chamber medium was determined. Bars represent mean ± SEM, N = 4, ** p<0.01 compared to MOI = 0 (one-way ANOVA). The basal medium was free of any culturable bacteria, as verified by plating 100 µl of the medium on BGA plates. (F) VA10 cell layers were infected as in (E) and the cellular cAMP levels were determined. Bars represent mean ± SEM, N = 4, * p<0.05, ** p<0.01 compared MOI = 0 (one-way ANOVA).

FIG 3: **CyaA-produced cAMP signaling causes disruption of tight junction complexes.** (A) VA10 cell layers were treated from the basolateral side with 500 ng/ml of CyaA for 1, 6, and 24 hours at 37 °C and the levels of mRNA for tight junction proteins were assayed by q-RT PCR; *UBC* was used as a reference gene. Bars represent the mean ± SEM, N = 3. (B) Cell layers were treated as described in (A), lysed, and probed by immunoblotting with antibodies recognizing the tight junction complex proteins. GAPDH was used as a loading control and the blots are representative of two independent experiments. (C) Cell layers were treated 500 ng/ml of CyaA, CyaA-AC$^-$, or TUC buffer from the basolateral side for 24 hours at 37 °C.

Confocal images of fixed cell layers were stained for the tight junction protein ZO-1 (green). The scale bar is 100 µm. Tight Junction Organizational Network rate (TiJOR) for the entire image was calculated for ZO-1 (B). Bars represent mean ± SEM of three experiments; * $p<0.05$ compared to TUC (one-way ANOVA).

Fig 4: **CyaA enhances mucin production in epithelial cell layers**. (A) 500 ng/ml CyaA, 1000 ng/ml CyaA-AC$^-$, or TUC buffer in DMEM/F12 was added to the basolateral side of VA10 cell layers for 3 or 24 hours at 37 °C. Relative expression of genes encoding mucin 5AC and mucin 5B were analyzed by q-RT PCR. Bars represent mean ± SEM of three experiments. *** $p<0.001$, **** $p<0.0001$ compared to TUC (one-way ANOVA). (B) Cell layers were treated with 500 ng/ml of CyaA, CyaA-AC$^-$, or TUC buffer for 24 hours as mentioned in (A) and the amounts of intracellularly accumulated mucin 5AC were measured by ELISA. Bars represent mean ± SEM of three experiments. * $p<0.05$ compared to TUC (students t-test). (C) Cell layers were treated as in (B), fixed, stained for the goblet cell marker mucin 5AC (red) and imaged by confocal microscopy. Scale bar is 100 µm. (D) Mean fluorescence intensity (± SEM) of mucin 5AC staining; N = 3, ** $p<0.01$ compared to TUC (one-way ANOVA).

FIG 5: **CyaA disrupts actin cytoskeleton in epithelial cell layers**. (A) Cell layers were treated as in Fig. 4C, fixed with paraformaldehyde and stained for F-actin with Alexa Fluor 488-phalloidin (green). Scale bar is 100 µm. (B) Mean fluorescence intensity (± SEM) of F-actin staining; N = 3, $p<0.05$ compared to TUC (one-way ANOVA).

FIG 6: **CyaA modulates expression of genes encoding antimicrobial peptides and cytokines/chemokines.** VA10 cell layers were treated from the basolateral side with

CyaA (500 ng/ml) in DMEM/F12 for 1, 6, and 24 hours; or TUC buffer. (A-L) Relative expression of genes encoding the antimicrobial peptides/proteins (A) Cathelicidin, (B) human beta defensin 1, (C) human beta defensin 2, (D) lysozyme, (E) secretory leukocyte peptidase inhibitor, (F) lactoferrin; and for the cytokines/chemokines (G) tumor necrosis factor-α, (H) interleukin-1α, (I) interleukin-1β, (J) interleukin-6, (K) interleukin-8, and (L) interleukin-10, were analyzed by q-RT PCR. *UBC* was used as a reference gene. Bars represent mean ± SEM, N = 3; ns indicates non-significant; *, $p< 0.05$; **, $p<0.01$; ***, $p<0.001$, ****, $p<0.0001$ compared to TUC control (one-way ANOVA).

FIG 7: **CyaA enhances secretion of IL-6, while inhibiting secretion of IL-8 and hBD-2 upon stiμlation by IL-17A.** VA10 cell layers were treated from the basolateral side with IL-17A (100ng/ml), CyaA (500 ng/ml), or both for 24 hours. IL-6 (A), IL-8 (B), and hBD-2(C) secretion levels were assayed from the basolateral supernatant by ELISA. Bars represent mean ± SEM of three replicates from a single experiment representative of 3 independent experiments.

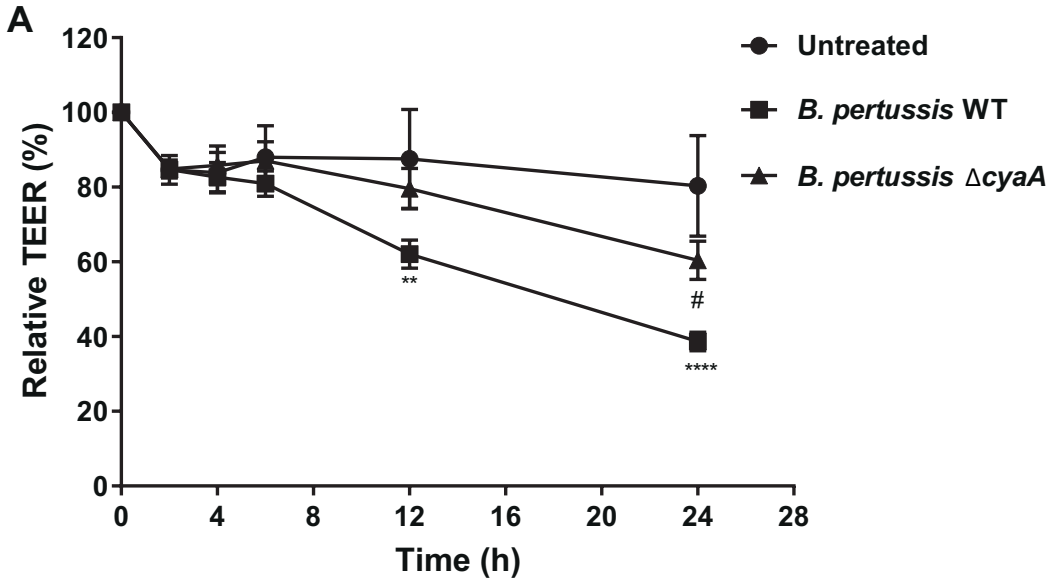
A
Relative TEER (%)
120
100
80
60
40
20
0
0
4
8
12
16
20
24
28
Time (h)
Untreated
B. pertussis WT
B. pertussis ΔcyaA
**
#
****

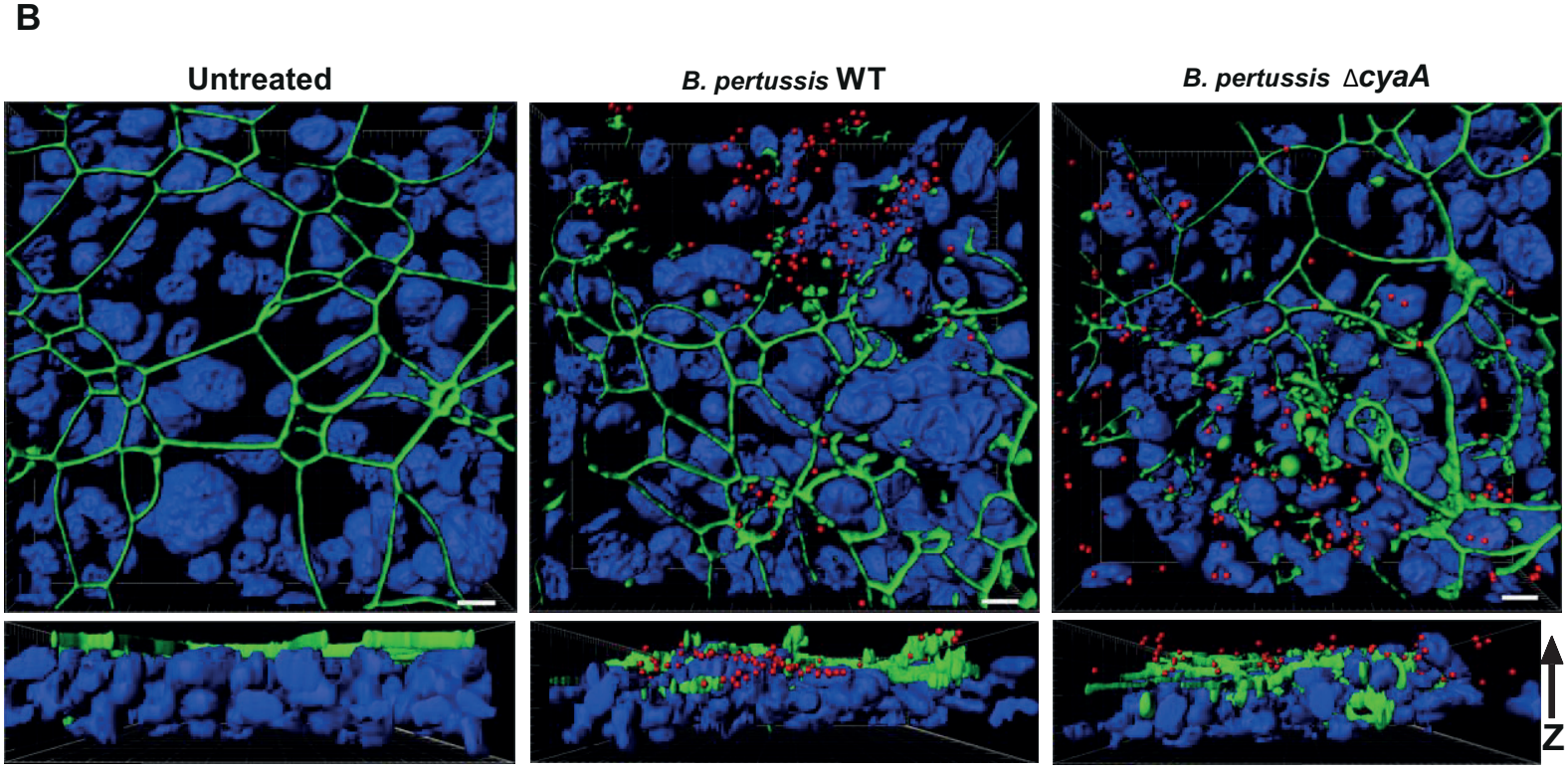
B
Untreated
B. pertussis WT
B. pertussis ΔcyaA
Z

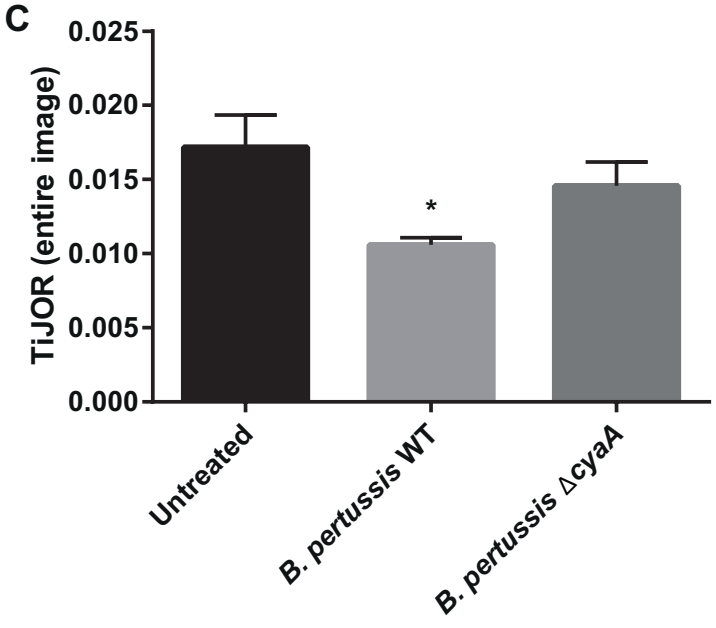
C
TiJOR (entire image)
0.025
0.020
0.015
0.010
0.005
0.000
*
Untreated
B. pertussis WT
B. pertussis ΔcyaA

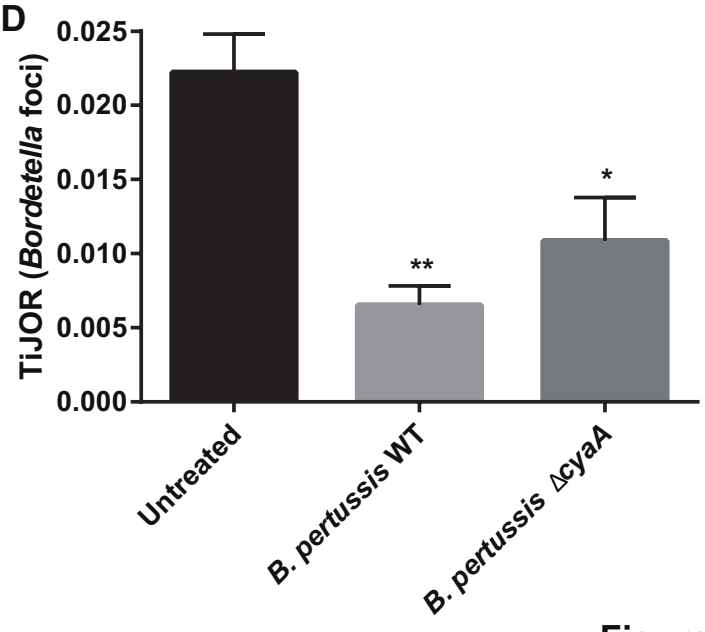
D
TiJOR (Bordetella foci)
0.025
0.020
0.015
0.010
0.005
0.000
**
*
Untreated
B. pertussis WT
B. pertussis ΔcyaA

Figure 1

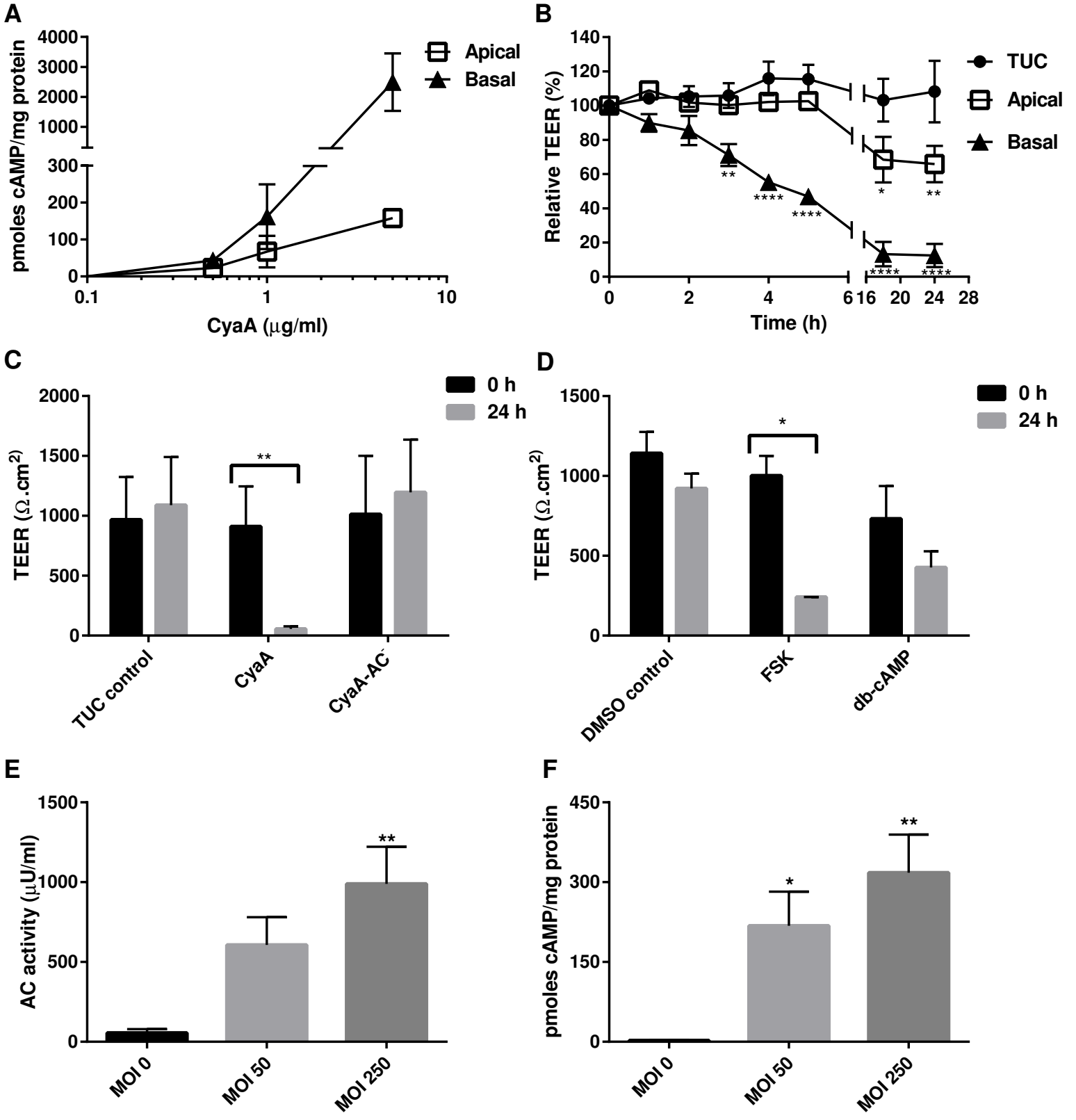
A
pmoles cAMP/mg protein
4000
3000
2000
1000
300
200
100
0
0.1
1
10
CyaA (μg/ml)
Apical
Basal
B
Relative TEER (%)
140
120
100
80
60
40
20
0
0
2
4
6
16
20
24
28
Time (h)
TUC
Apical
Basal
**
****
****
*
**
****
****
C
TEER (Ω.cm2)
2000
1500
1000
500
0
**
0 h
24 h
TUC control
CyaA
CyaA-AC
D
TEER (Ω.cm2)
1500
1000
500
0
*
0 h
24 h
DMSO control
FSK
db-cAMP
E
AC activity (μU/ml)
1500
1000
500
0
**
MOI 0
MOI 50
MOI 250
F
pmoles cAMP/mg protein
450
300
150
0
*
**
MOI 0
MOI 50
MOI 250

Figure 2

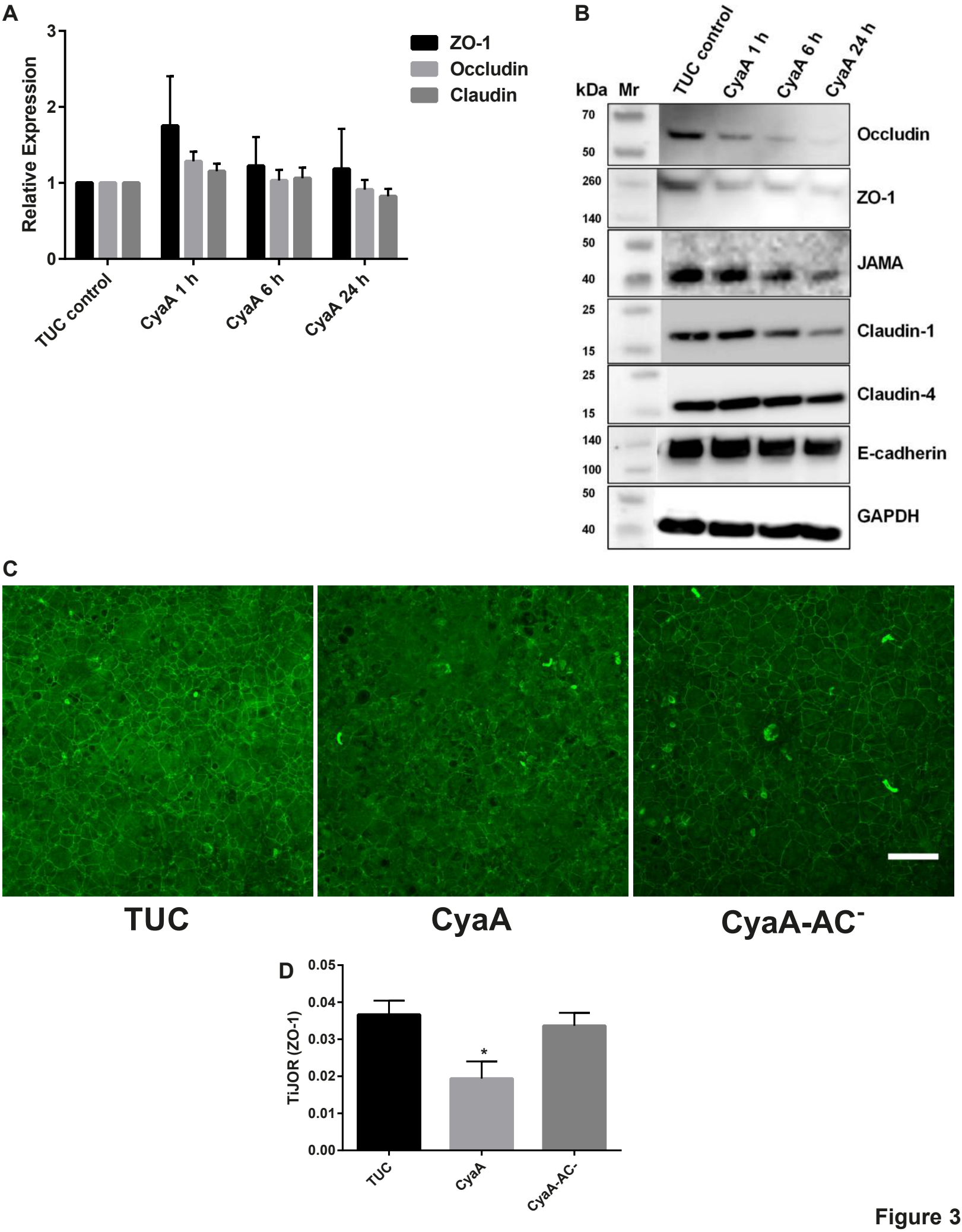
A
Relative Expression
3
2
1
0
ZO-1
Occludin
Claudin
TUC control
CyaA 1 h
CyaA 6 h
CyaA 24 h
B
kDa
Mr
TUC control
CyaA 1 h
CyaA 6 h
CyaA 24 h
70
50
Occludin
260
140
ZO-1
50
40
JAMA
25
15
Claudin-1
25
15
Claudin-4
140
100
E-cadherin
50
40
GAPDH
C
TUC
CyaA
CyaA-AC-
D
TiJOR (ZO-1)
0.05
0.04
0.03
0.02
0.01
0.00
*
TUC
CyaA
CyaA-AC-

Figure 3

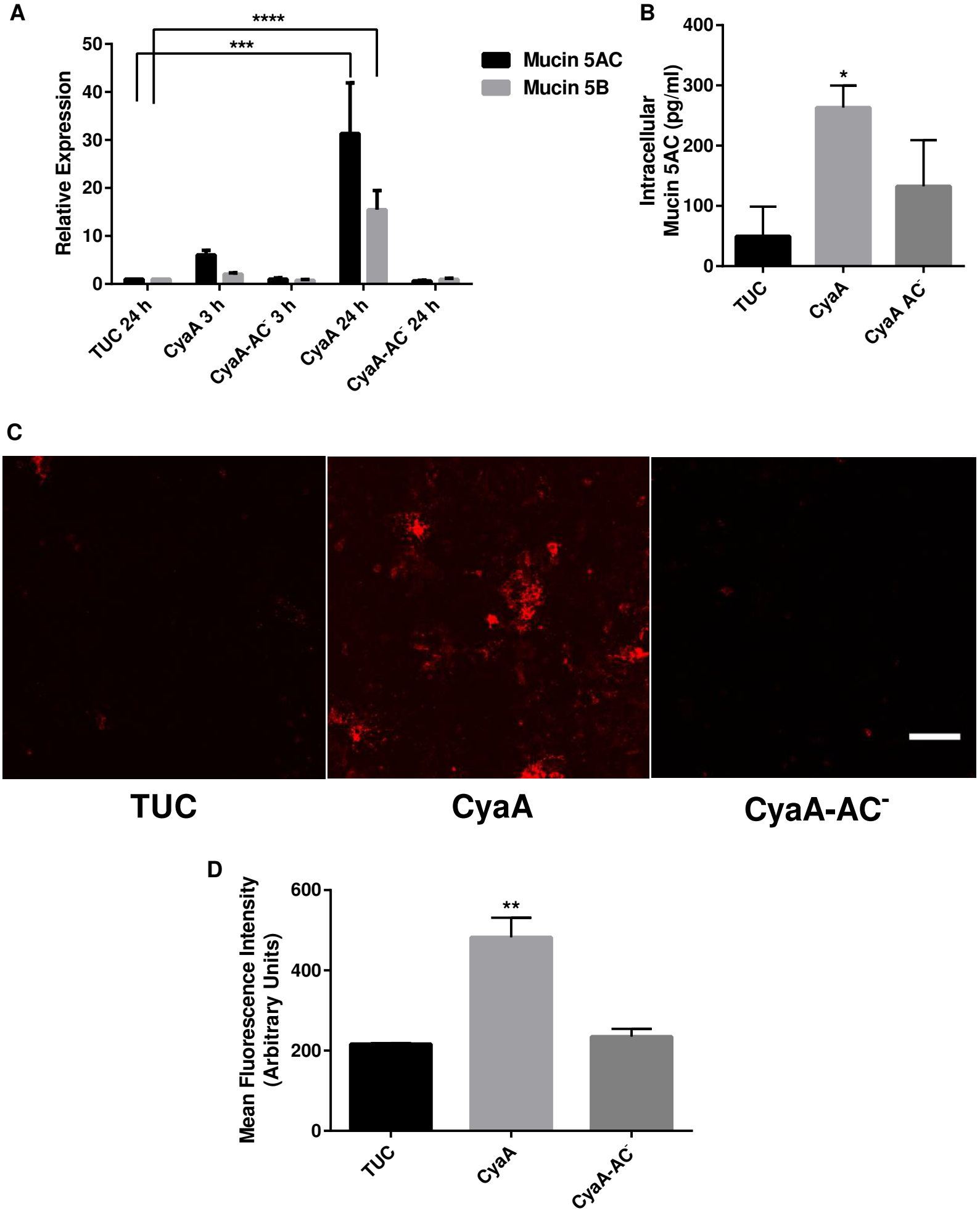
A
****
***
Relative Expression
50
40
30
20
10
0
Mucin 5AC
Mucin 5B
TUC 24 h
CyaA 3 h
CyaA-AC- 3 h
CyaA 24 h
CyaA-AC- 24 h
B
Intracellular Mucin 5AC (pg/ml)
400
300
200
100
0
*
TUC
CyaA
CyaA AC-
C
TUC
CyaA
CyaA-AC-
D
Mean Fluorescence Intensity (Arbitrary Units)
600
400
200
0
**
TUC
CyaA
CyaA-AC-

Figure 4

A

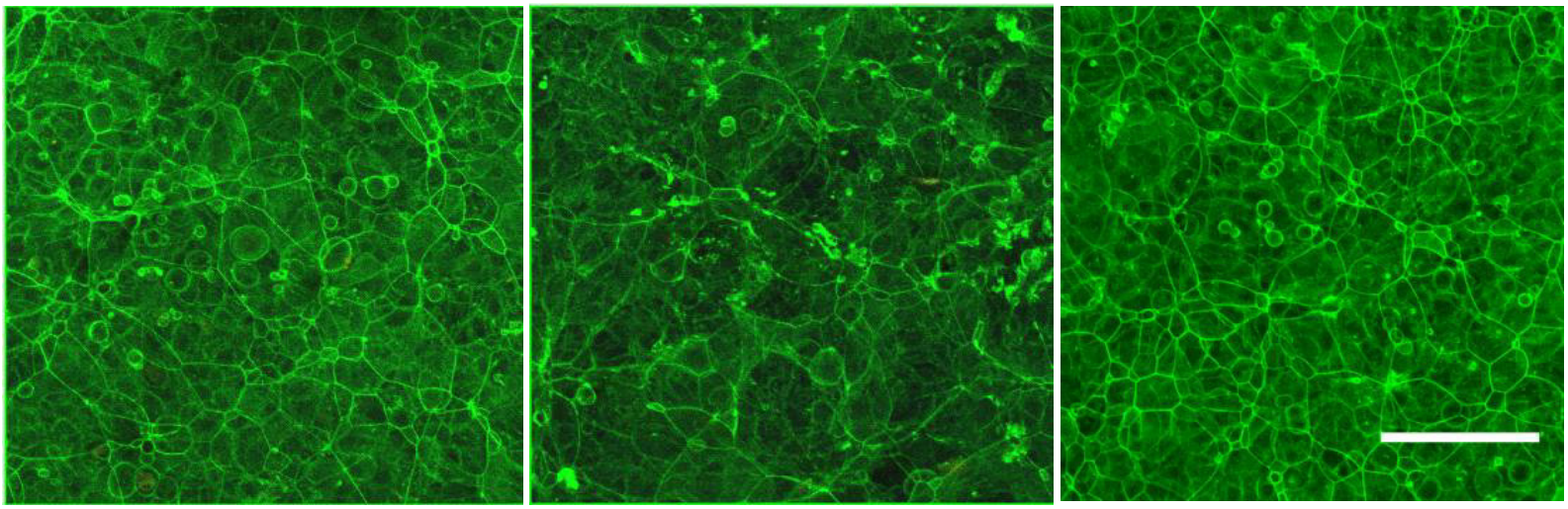

TUC CyaA CyaA-AC$^-$

B

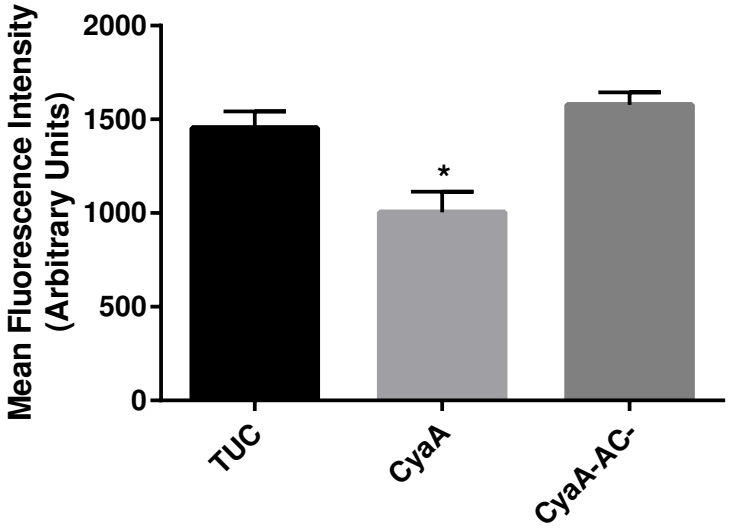

Figure 5

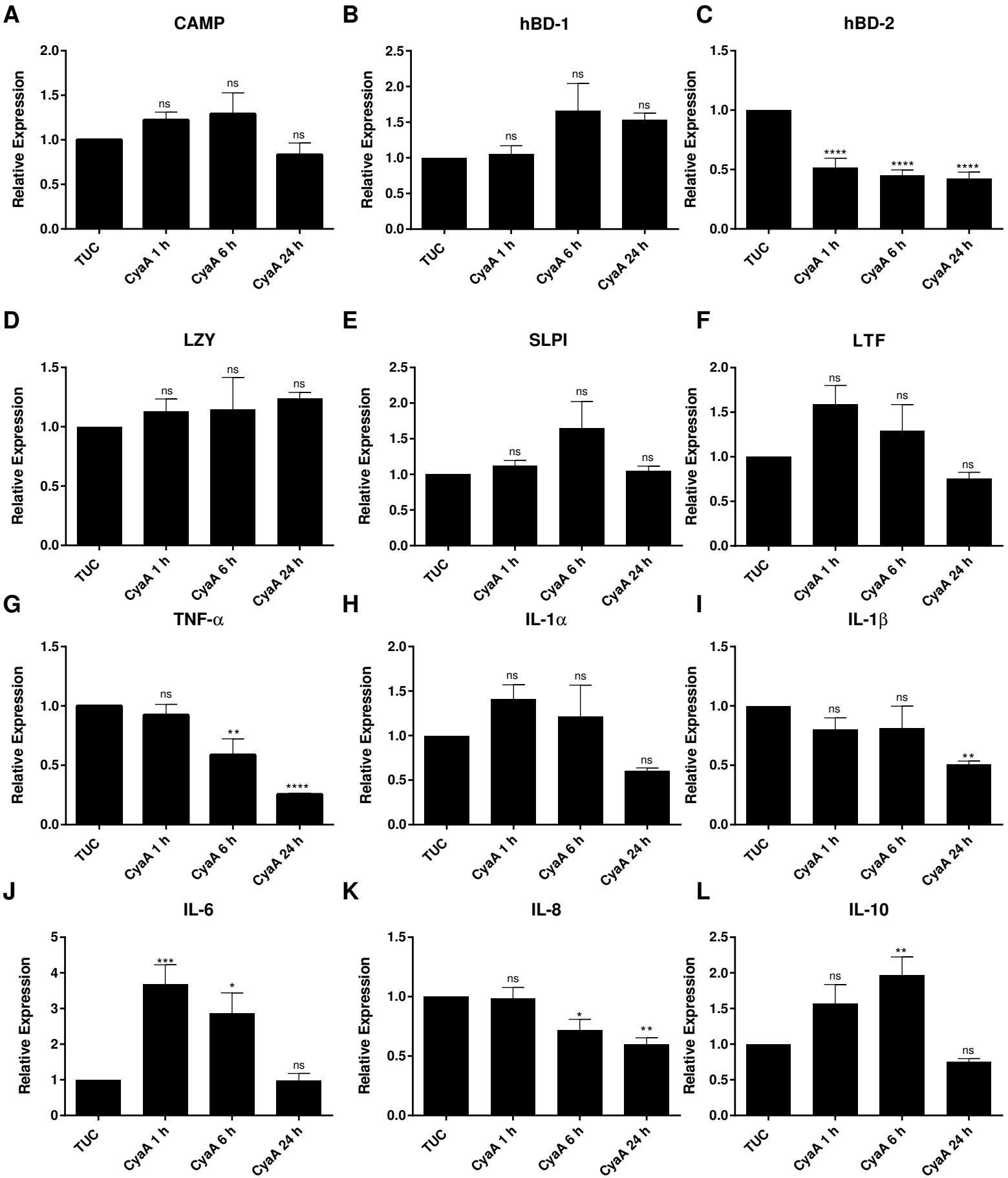
A
CAMP
B
hBD-1
C
hBD-2
D
LZY
E
SLPI
F
LTF
G
TNF-α
H
IL-1α
I
IL-1β
J
IL-6
K
IL-8
L
IL-10
Relative Expression
TUC
CyaA 1 h
CyaA 6 h
CyaA 24 h
ns
*
**
***
****

Figure 6

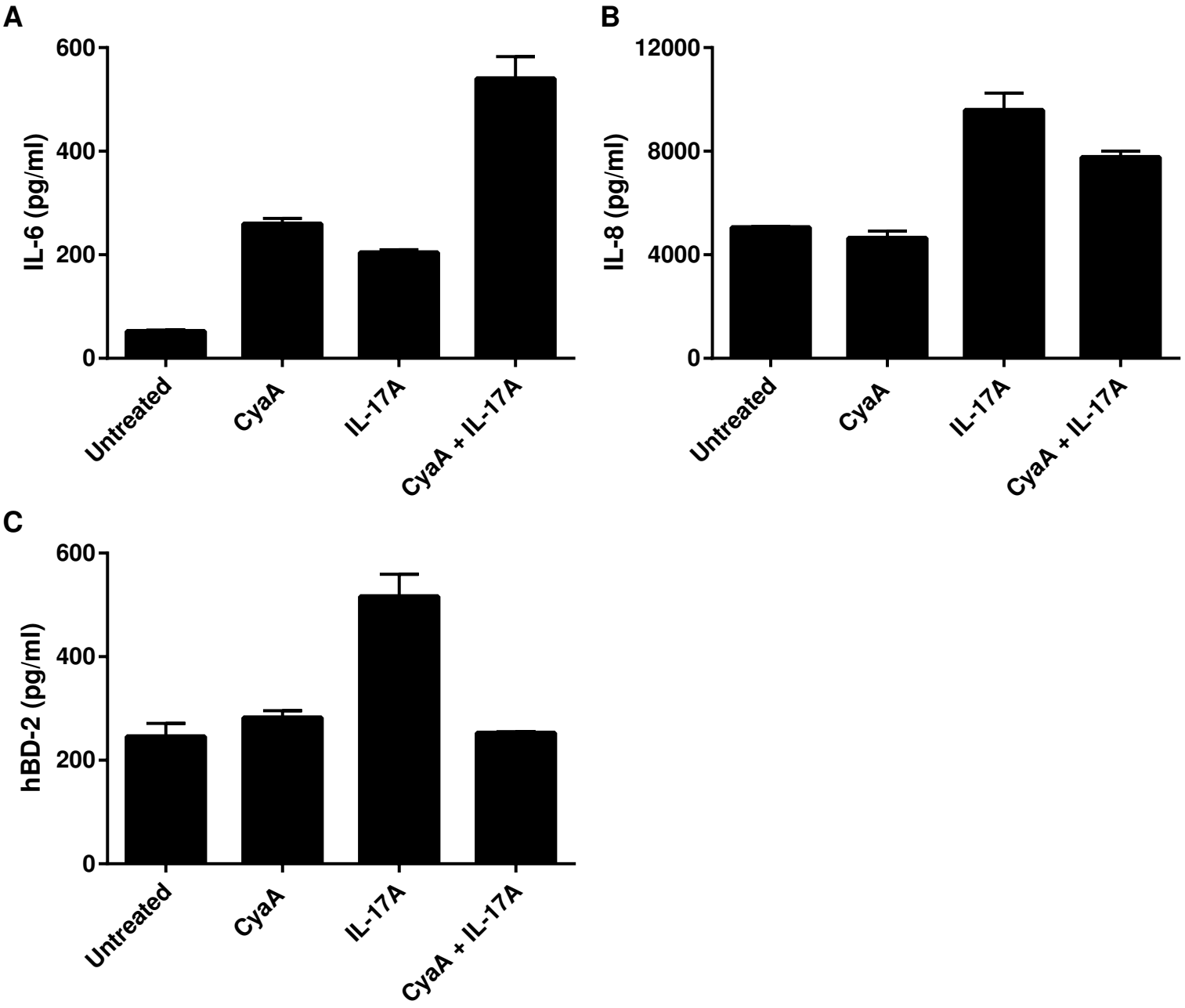
A
600
400
200
0
IL-6 (pg/ml)
Untreated
CyaA
IL-17A
CyaA + IL-17A
B
12000
8000
4000
0
IL-8 (pg/ml)
Untreated
CyaA
IL-17A
CyaA + IL-17A
C
600
400
200
0
hBD-2 (pg/ml)
Untreated
CyaA
IL-17A
CyaA + IL-17A

Figure 7